SYNTHESIS OF STRONTIUM DOPED IRON OXIDE NANOPARTICLES FOR DRUG DELIVERY APPLICATIONS

By

Imad Ud Din

School of Chemical and Materials Engineering

National University of Sciences and Technology

2023

SYNTHESIS OF STRONTIUM DOPED IRON OXIDE NANOPARTICLES FOR DRUG DELIVERY APPLICATIONS

Name: Imad Ud Din

Reg no:00000330123

This thesis is submitted as a partial fulfillment of the requirements for the degree of

MS in Materials & Surface Engineering

Supervisor: Dr. Usman Liaqat

School of Chemical and Materials Engineering (SCME)

National University of Sciences and Technology (NUST)

H-12 Islamabad, Pakistan

February, 2023

Dedication

I dedicate this thesis to My Parents & My Respected Teachers without whom I would not be here. Thanks for their endless Guidance and Support

Acknowledgments

I would like to acknowledge and give my warmest thanks to my supervisor **Dr Usman Liaqat** who made this work possible. His guidance and advice carried me through all the stages of writing my project. I would also like to thank my committee members for letting my defense be an enjoyable moment, and for your brilliant comments and suggestions, thanks to you.

I would also like to give special thanks to my family as a whole for their continuous support and understanding when undertaking my research and writing my project. Your prayers and assistance for me was what sustained me this far.

Finally, I would like to thank Almighty Allah, for letting me through all the difficulties. I have experienced your guidance day by day. You are the one who let me finish my degree. I will keep on trusting you for my future.

Abstract

Iron oxide nanoparticles has been one of the most researched materials for biomedical application, especially drug delivery due to its incomparable properties like magnetic nature (superparamagnetism), biocompatibility, availability (abundance) and ease of synthesis. This research focuses on the synthesis of magnetite nanoparticles and strontium doped Iron oxide nanoparticles for drug delivery applications through hydrothermal and coprecipitation route. Ibuprofen is used as an anticancer drug which is loaded on these bare nanoparticles (Fe_3O_4 and strontium doped Iron oxide nanoparticles). These prepared nanoparticles were characterized by X-ray powder diffraction (XRD), Scanning electron microscopy (SEM), Energy dispersive X-ray (EDX), Fourier-transform infrared spectroscopy (FTIR), Vibrating Sample Magnetometer (VSM) and UV Vis spectroscopy (UV). Drug loading is characterized by UV-vis Spectroscopy whereas cytotoxicity of both nanoparticles and drug loaded nanoparticles are analyzed by MTT Assay. XRD results showed formation of both magnetite and strontium doped Iron oxide nanoparticles and showing the relevant peak of synthesized nanoparticles both by hydrothermal and Coprecipitation method. SEM results confirmed formation of nanoparticles below 100 nanometer (nm) for both Fe_3O_4 and strontium doped Iron oxide nanoparticles, desired for biomedical applications (drug delivery). EDX results confirmed step by step (increasing) doping of strontium in Iron oxide phase by highlighting increased atomic and weight percent of strontium in results. VSM results confirmed the formation of single domain structure. FTIR showed presence of Ibuprofen molecules on the surface of molecule and also confirmed the formation of desired material. Increased drug loading was observed in case of strontium doped iron oxide nanoparticles (0.25 mole strontium doped) which showed maximum encapsulation efficiency of 44.01% which was more than of Fe_3O_4 nanoparticles encapsulation efficiency of 34.31%. Strontium doped Iron oxide nanoparticles showed better drug release profile than Iron oxide nanoparticles. Cytotoxicity test showed increase in cytotoxicity with increase in the concentration of nanoparticles from 300 µg/ml to 500 µg/ml for both magnetite and Strontium doped Iron Oxide nanoparticles. Ibuprofen loaded nanoparticles showed more cytotoxicity with respect to non-loaded nanoparticles at same concentration for both magnetite and strontium doped Iron oxide nano particles.

Table of Contents

List of Figures:

List of Tables:

List of Abbreviations:

EDX	**Energy Dispersive X-Ray**
SEM	**Scanning Electron Microscope**
XRD	**X-ray Powder Diffraction**
FTIR	**Fourier-Transform Infrared Spectroscopy**
SPIONs	**Superparamagnetic Iron Oxide Nanoparticles**
nm	**Nanometers**
BIM	**Biologically Induced Biomineralization**
BCM	**Biologically Controlled Biomineralization**
CVD	**Chemical Vapor Deposition**
PVD	**Physical Vapor Deposition**
MNPs	**Magnetic Nanoparticles**
RES	**Reticuloendothelial System**
MRI	**Magnetic Resonance Imaging**
NSAID	**Non-Steroidal Anti-Inflammatory Drugs**
MTT	**(3-(4,5-Dimethylthiazol-2-yl)-2,5-Diphenyltetrazolium Bromide)**
DMSO	**Dimethyl Sulfoxide**
HMEM	**Hank's Minimum Essential Medium**
EE	**Encapsulation Efficiency**
CC	**Cumulative Concentration**
FDA	**Food and Drug Administration**

Chapter 1:

Introduction

One of the most significant areas of researches in current science is nanotechnology as it allows researchers, scientist and engineers to work at molecular and cellular level. Nanoparticles are the organic or inorganic materials, having at least on size dimension in range of 1 to 100 nanometer(nm)[1], have enhanced properties as compared to their bulk counterparts. Nano materials are basically divided with respect to their dimension including zero dimension characterized as quantum dots, one dimension as wires and rods at nano scale, two dimensional nano materials include nano films, nanolayers and nanocoating like graphene and three dimension includes belts, sheets, disks and films at nanoscale. Due to their superior optical, catalytic, electric and magnetic properties nanoparticles are getting great attention. Nanoparticles in such size range are faster (faster clearance and diffusion), lighter in weight, can get into smaller spaces, cheaper and are more energy efficient. Nanoparticles at this size range enhances adsorption, absorption and penetration due to improved interaction at molecular level. The change in properties at nanoscale are due to two main reasons. Firstly, the surface area to volume ratio increases as most of the atom become nearer to the surface hence making them weakly bonded and make them more reactive. Secondly there is a change in electric and optical properties of the material which in due to quantum mechanical effect in which size of the structure become relatable to the wavelength of the electron which results in quantum confinement and hence change in optical and electronic properties can be seen. Due to these reasons we can see enhanced properties like reduce in melting point, increase in hardness, changed optical, electrical and magnetic properties, self-purification process can be seen and due to increase in perfection chemical stability can be seen. Due to excellent properties of these nanoparticles unusual increase in their use in life sciences can be seen. Nanotechnology introduces various applications int the field of biomedical. These applications include drug delivery, magnetic hyperthermia, Bio imaging, sensors (bio sensors) and various other applications. Nano technology majorly focuses on therapeutic and diagnostic applications in the felid of biomedical science as done in previous researches [2][3][4][5][6].

1.1 Synthesis of Nanoparticles:

Nano particles can be synthesized using various techniques. These techniques can be divided into three major categories including physical, chemical and biological methods[7]. In physical methods we synthesize nanoparticles using techniques like gas phase deposition, pulse lase ablation, electron beam lithography, laser induced pyrolysis and power ball milling techniques. Chemical methods include techniques like coprecipitation, microemulsion, hydrothermal and sol gel methods. Biological methods include green synthesis of nanoparticles using bacteria fungi or protein extracts. The method is chosen on the basis of desired shape, size, distribution, purity and quantity of end nano-product. The following details of synthesis includes:

1.1.1 Physical Methods:

1.1.1.1 Physical Vapor Deposition (PVD)/Chemical Vapor Deposition (CVD):

PVD and CVD are basically part of gas phase deposition technique in which the particles are supersaturated from gas phase onto the substrate. The process is done in inert atmosphere which leads to production of fine powders or thin films without any contamination. The precursors are evaporated in a chamber filled with inert gas and at higher atmospheric pressure. The precursors collide with inert gas and lose their energy hence condensing into nanocrystals through the phenomenon of Brownian gelling and combination [8]. The particles produced through gas phase are much pure and there is no contamination as compared to liquid phase deposition technique [9]. Through this technique the particles can be synthesized on bulk scale. The drawback of this technique is that the size of the nanoparticles cannot be maintained throughout the experiment.

1.1.1.2 Electron Beam Lithography:

In this technique a beam of electron is emitted on a substrate of the material whose nanoparticulate are desired. The emitted electron beam removes the exposed or non-exposed area of the substrate surface which is usually immersed in a water bath which evaporates the material creating nanoparticle below 50 nanometer size[9]. This technique

gives us small size nanoparticles but consist of disadvantages like high production cost and having long process time making it uneconomical.

1.1.1.3 Pulse Laser Ablation:

In this technique conditions like temperature, pressure, density etc. can be controlled effectively with respect to other physical methods. In this process the material is removed from the target using a pulse laser beam[10]. This process produces a plasma cloud at higher temperature and pressure which react with the ablated material to form metastable nanoparticle through the course of nucleation and growth[11]. The positive aspect of this process is that it is environment friendly as no harm to the environment by the byproduct formed[12]. Despite having many positive aspects, the process has drawbacks like sputtering and inhomogeneities in the energy profile of the plume[13].

1.1.1.4 Pyrolysis Induced By laser:

In this process a laser is used to head a gaseous mixture of precursors of nanoparticles which produces scattered nanoparticles[14]. In this process the parameters are varied like fuel to air ratio and vapor pressure of the precursors which produces nanoparticles in size below 7 nanometers[15]. The techniques have a drawback of difficulty in controlling size of final particles therefore we get a broad range of size distribution of these nanoparticles.

1.1.1.5 Ball Milling:

In this method the precursor powder is milled in a jar with the help of metallic balls (e.g. Tungsten carbide balls). The phenomenon of cold welding and fracture occurs during the whole process and fine and uniformly dispersed powder is obtained[15]. The size highly depends upon mills rotation time and speed. Industrial scale production of nanoparticles is possible through ball milling technique[16][18]. Agglomeration is a drawback of this technique which can be overcome by using surfactants or ultrasonication of particles[17]**.**

1.1.2 Chemical Methods

1.1.2.1 Coprecipitation:

It the process in which precursors are reduced using a reducing agent and nanoparticles are obtained under the condition of supersaturation. It is the simplest and widely used technique for the synthesis of nanoparticles. It includes collective existence of nucleation, growth and coarsening[19]. Nucleation is the key step in this process. In this technique nanosized particles are precipitated out of a continuous solvent. Metallic salts that are inorganic in nature are dissolved in a solvent[20]. These metallic salts act as metal hydrates species which is reduced by a basic solution creating a condition of super saturation and nanoparticles are precipitated out. Change in ph., ionic strength and amount of reducing agent can be used to control particle size and shape[21].

1.1.2.2 Hydrothermal Technique:

It is a process in which reactants are dissolve in a solvent within a closed vessel known as autoclave. The vessel is heated under high pressure and above solvent boiling temperature. Basic solvent is desirable as their solubility increases dramatically with increase in temperature[22]. Good control over size shape and crystallinity can be achieved through this process. The drawbacks of this process are expensive equipment and safety issues during reaction as chances of autoclave explosion if not handled properly.

1.1.2.3 Sol Gel:

Sol can be described as colloidal solution made up of particles suspended in liquid phase whereas gel can be defined as solid macromolecule in a solvent. Therefore, it is a process in which a liquid with precursors is converted to gel and with further treatment is converted to its solid oxide material. It is a process in which molecular precursors are converted into oxide network through polycondensation process. The idea behind is to dissolve compound in a solvent and bring it to back to solid in a controlled manner. This process allows mixing in at atomic scale. Dense powder, thin films, porous structures and fibers can be synthesized through this technique[23].

1.1.2.4 Microwave Assisted Synthesis:

This process is based on the interaction of microwave, ranging from 300 Mhz to 300 Ghz, and precursor material on dipole interaction and ionic conduction mechanism. Heat is generated by dipole interaction when polar end of molecules oscillates with oscillating electric field hence generating heat. This process is faster than traditional chemical reactions, have higher yield and less biproducts. It can selectively heat either the solvent or precursor material for the synthesis of nanomaterial[24].

1.1.2.5 Sono-Chemical Synthesis:

In this process acoustic cavitation is caused due to irradiation caused by ultrasonic waves. This generated bubbles in the solvent which grows and implode causing hot areas of high temperature and pressure. It is a method in which we can synthesized nanoparticles with controlled morphologies in lesser time. The disadvantage of this process is that it is an energy intensive process[25].

1.1.3 Biological Methods:

Nanoparticles can be synthesized using biotic species like bacteria, protein and plants extract. In this synthesis technique nanoparticle are synthesized using process like Biologically induced Biomineralization (BIM) and Biologically controlled biomineralization (BCM)[26]. In BCM, nanoparticles are synthesized naturally using environmental parameters like temperature, redox potential, partial pressure of oxygen and carbon dioxide and ph. This is an extracellular type of synthesis for nanoparticles. If the synthesis of nanoparticles is done through the process of bacteria reduced by Sulphur then the process is known as biologically controlled biomineralization. The process occurs in absolute geochemical environment as the whole process occurs at a specific site, like within cell wall or cytoplasm, completely separating it from the external environment hence making a much-controlled process giving us a better morphology and size of end nanoparticles. Although biological synthesis of nanoparticles is a green synthesis method, then end particles are not monodispersed and the synthesis process is

slow[27]. The summary of advantages and disadvantage of the following synthesis techniques are summarized below in the table.

Table 1: Summary of advantages and dis advantages of nanoparticles synthesis techniques

Method	Advantages	Disadvantages
PHYSICAL METHOD		
Gas Phase Deposition	• Fine powder is produced • High purity	• Inability to maintain size of nanoparticles throughout the experiment • Controlled and expert approach in required
Electron Beam Lithography	• Produces fine size nanoparticles (<50nm)	• High production cost • Lengthy process • Resolution limitations
Pulse Laser Ablation	• Fast, Simple, Cost effective • Controlled parameters like pressure, temperature and density	• High kinetic energy causes re-sputtering causing inhomogeneous energy distribution of laser beam
Laser-Induced Pyrolysis	• Produce particles less than 10 nanometers	• Difficulty in obtaining uniformity • Broad size distribution of end particles is obtained
Ball Milling	• Nanoparticles with good dispersion is obtained • Nanoparticles can be synthesized on industrial scale	• Agglomeration due to fine particles interaction
CHEMICAL METHODS		
Coprecipitation	• Simple process • Ambient working conditions • Can control particle size	• Reactants with different precipitation rate are difficult to work with in this process • Impurities may also get precipitated during the reaction
Hydrothermal	• Precise control on size shape, crystallinity and distribution of final product • Significantly enhanced chemical reactivity of reactants	• Expensive autoclaves required • Un-safe reaction process.

Sol Gel	• Uniform mixing of precursors at molecular level • High purity products • Better control over product final composition • Controlled porosity can be obtained	• Longer reaction time • Harmful organic solvents
Microwave Assisted	• Faster chemical reactions • Higher yields • Lesser side products	• Expensive equipment • Difficult to scale up • Difficult monitoring of reaction
Sono-Chemical Synthesis	• Ambient temperature synthesis of nanomaterials • High reaction rate and lesser reaction time • Simple method	• Energy intensive process • Difficult to scale up • technique not for heat sensitive material
Biological Methods	• Green synthesis process	• Lower yield • Slow reaction rates

1.2 Magnetic Nano Particles (MNPs):

Applications of MNPs are growing faster nowadays. Having size ranging from 1nm to 100 nm, make these nanoparticles distinguishable from there bulk counterpart. MNPs have properties like high surface area, high magnetization values, metal enriched constituents, Chemical stability, ability to be surface functionalized, application at molecular and cellular level and biocompatibility make them suitable for various application in the field of biomedical science. Properties of MNPs can be controlled by changing its physiochemical properties and can be applied to various fields. There (synthesized nanoparticles) size and shape strongly depend upon synthesis conditions and surfactants used which plays an important role in synthesizing nanoparticles of monodispersed nature. These nanoparticles can be used in applications like biomedicine, environmental fields and agriculture. MNPs are made up of different metal element and metal oxides having magnetic properties.

The composition of nanoparticles can be comprised of different types including mono-components comprising of nanoparticles based on Fe, Ni and Co having good magnetic properties[28]. In these nanoparticles Iron is mostly studied due to its chemical stability, Biocompatibility and environmental friendly nature, metal alloys based nanoparticles

including Iron platinum (FePt) and Iron palladium (FePd) nanoparticles having high magnetic crystallinity and chemical stability, metal oxide based nanoparticles majorly comprising of magnetite nanoparticles having high magnetization values, biocompatibility and chemical stability[29] , metal carbides nanoparticles comprising of nanoparticles based on iron carbide including Fe5C2, Fe3C and Fe2C. It also includes heterostructure magnetic nanoparticles containing nanostructure like FePt-Au magnetic structures which exhibits excellent magnetic properties[30]. Majorly Iron oxide nanoparticle are used in biomedical application due to their superior properties like high magnetic saturation, good stability and minimal toxicity. Maghemite ore of iron oxide is more stable in aqueous media give more magnetic character. Iron oxide nanoparticle of size above 50 nm is known as superparamagnetic and whereas below 50nm it is known as ultra-small superparamagnetic. Magnetic ferrites having general formula of MFe_2O_4, having spinal structure, are extensively studied due to their biomedical applications. The 'M' in the MFe_2O_4 represents material like zinc, manganese, Cobalt, Nickel and magnesium etc.[32]. These materials help in improving magnetic properties of magnetic core of iron oxide. Magnesium or cobalt doping aids in the betterment of magnetic properties of iron oxide by improving magnetic resonance signals by magnesium addition and improving specific absorption rate by the addition of cobalt [29][31]. Some of these nanoparticles with their biomedical applications are given below.

Table 2:Summary of Nanomaterials with properties favorable to biomedical applications

Material Category	Nano Particles	Properties
Metallic	**Gold (Au)**	• Chemical inertness • Ability of surface functionalization • Negative charge on its surface
	Silver (Ag)	• High electrical conductivity • Thermal conductivity • Chemical stability • Catalytic activity • Antibacterial • Enhanced optical properties
Bi-Metallic	**FePt**	• Chemical stability • super Para magnetisation • High Curie temperature • High saturation magnetization • High X-ray absorption
	FeCo	• Super Para magnetism • high Curie temperature • High saturation magnetization

	FeNi	• High Curie temperature • High saturation magnetization
	CuNi	• Good Curie temperatures • Magnetic properties
Magnetic	Fe_3O_4	• Chemical Stability • Nontoxicity • Biocompatibility • High saturation magnetization • High magnetic susceptibility
	Co-Fe2O4	• High magneto-crystalline anisotropy • High coercivity • High curie temperature • Moderate magnetization saturation • Chemically stable
	Mn-Fe2O4	• High magnetization • Magnetic susceptibility • Large relativities • Biocompatible.

1.3 Magnetism

Magnetic nanoparticles can be manipulated using external magnetic field as their properties are strongly anchored by the morphology, size, surface functionalities and magnetization values. Magnetic nature of nanoparticles is characterized by their electrostatic forces produced by orbital and spinning motion of electrons and their interactions. The response of a material to a magnetic field is known as magnetic susceptibility meaning how much a material is magnetized in presence of a magnetic field. The ability of a material to retain magnetism in the absence of magnetic field is known as remanence and the total amount of magnetization required to completely demagnetize the magnetic material is known as coercivity.

Magnetic materials are characterized on the basis of their magnetic moment's magnetic susceptibility and orientation which are described below.

1.3.1 Diamagnetic Material:

These are the materials when placed under external magnetic field they get weakly repelled by that magnetic field and get magnetized in the opposite direction of applied magnetic field having weak and negative susceptibility value. When placed in a magnetic field the magnetic field lines are repelled from the center of diamagnetic material. When placed under nonuniform field the diamagnetic material moves form strong field region

to weak field region. These material losses magnetization when external magnetic field is removed due to no unpair electrons. These materials could be in a form of water liquid and gas. Examples includes hydrogen, mercury, water, copper and gold.

1.3.2 Paramagnetic Material

These are the materials when placed under external magnetic field they get weakly attracted by that magnetic field and get magnetized in the same direction of applied magnetic field having weak and positive susceptibility value. When placed in a magnetic field the magnetic field lines are attracted to the center of Paramagnetic material. When placed under nonuniform field the paramagnetic material moves form weak field region to strong field region. These material losses magnetization when external magnetic field is removed but have some unpaired electrons. These materials could be in a form of water liquid and gas. Examples includes Aluminum, platinum, sodium and crown glass.

1.3.3 Ferromagnetic Material:

These are the materials when placed under external magnetic field they get strongly attracted by that magnetic field and get magnetized in the same direction of applied magnetic field having strong and positive susceptibility value. When placed in a magnetic field the magnetic field lines are strongly attracted to the center of ferromagnetic material. When placed under nonuniform field the ferromagnetic material moves form weak field region to strong field region. These materials retain magnetization when external magnetic field is removed and can act as a magnet and have unpaired electrons. These materials could only be in a form of gas. Examples includes Iron, cobalt, Nickel.

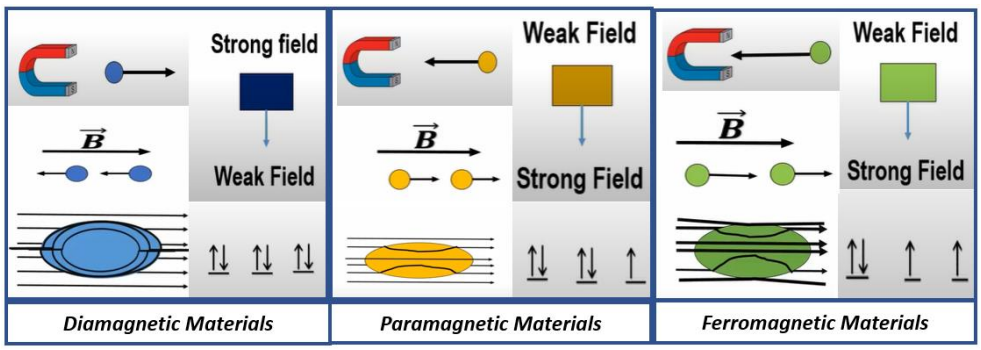

Figure 1: Different groups of magnetic materials

1.3.4 Ferrimagnetic Material:

These are the material in which magnetic domains are aligned in both parallel and anti-parallel direction in unequal numbers so they are unable to cancel out each other. This occurs as the sublattices are separated by oxygen ions. These materials are weakly attracted by magnetic field. Examples include Fe_3O_4, MgFe2O4, ZnFe2O4 etc. These materials sometimes loose there ferrimagnetic property and changes to paramagnetic material.

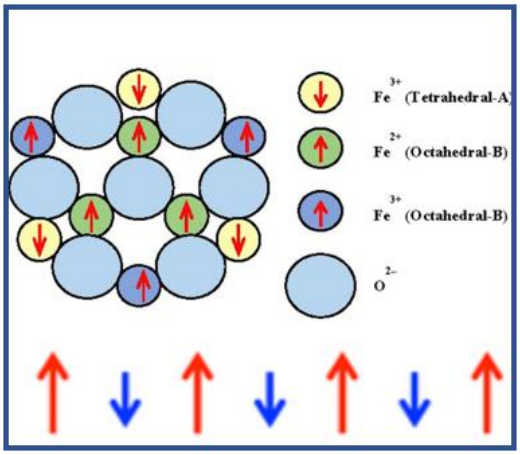

Figure 2 Ferromagnetic materials domains

1.3.5 Anti-Ferromagnetic Material:

In this type of material adjacent dipoles are arranged in anti-parallel manner with same magnitude. Susceptibility is very small and positive and it is usually dependent on temperature. The susceptibility increases until Neel temperature and after that susceptibility decreases. Examples of these material are MnO, MnS, Cr2O3 and NiCr etc.

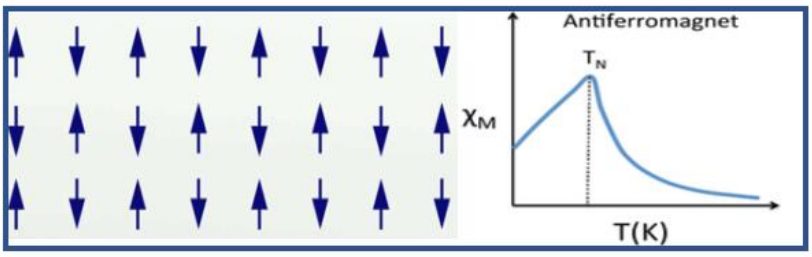

Figure 3: Anti-ferromagnetic domains

1.3.6 Super Para Magnetic Material:

Phenomenon of superparamagnetism occurs when the particle size is below a critical particle size below which particle have single domain making them superparamagnetic. In this size materials coercivity, remanence and hysteresis become zero. The logic behind this is that as the particle size decreases the anisotropy energy decreases which results in decrease in coercivity. As the size decreases volume dependent anisotropy decreases and becomes comparable to thermal energy and time come when thermal energy become greater which eventually results in filliping of magnetization with high frequency form one direction to another even in the absence of magnetic field which results in the phenomenon of superparamagnetism[36].

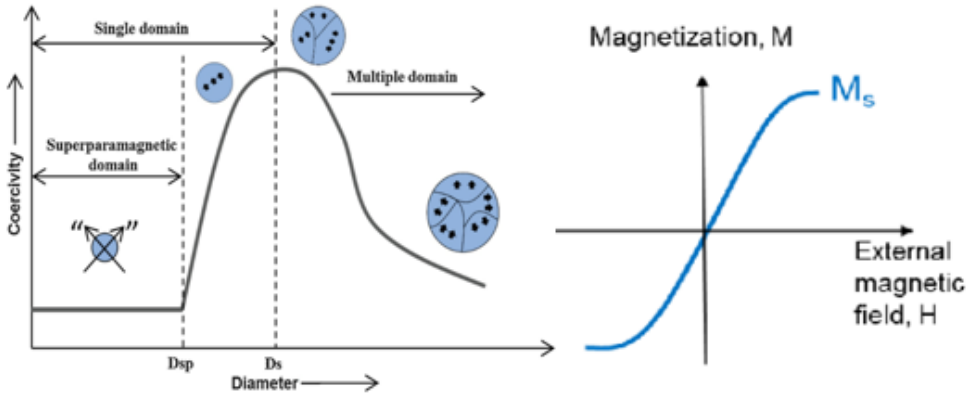

Figure 4: Superparamagnetic materials behavior, Hysteresis loop

1.4 Iron Oxide Nanoparticles:

Due to its incomparable physical and chemical properties nanotechnology has gained noteworthy interest of researchers. Nanoparticles have properties like large surface area to volume ratio, biocompatibility, high surface functionality and bioactivity, which are absent from bulk scale, making them more attractive for practical application in the field of biomedicine. Iron oxide nanoparticles have been studied extensively due to its inherent magnetic properties (showing superparamagnetic behavior) making them suitable for biomedical, electronics and environmental applications. In addition to these properties, properties like biocompatibility, stability and being environmentally friendly makes them

suitable for biomedical applications. Biomedical applications of Iron oxide nanoparticles include the use of iron oxide nanoparticles as MRI contrast agents, use in magnetic hyperthermia treatment, targeted drug delivery, invitro bio separation, tissue engineering, Radiography, and ecological remediation. Iron oxide nanoparticles can be synthesized by various methods including physical, chemical and biological. The physical methods include power ball milling, gas-phase deposition, pulsed laser ablation synthesis techniques. Chemical methods majorly include hydrothermal, chemical co-precipitation, and micro-emulsions synthesis techniques. Nanoparticles are synthesized by using bacteria and plants in biological synthesis techniques.

1.5 Applications of Iron Oxide Nanoparticles:

Major research in the field of nanotechnology in biomedical applications is regarding drug delivery. Cancer treatment are majorly done by chemotherapy which basically rely on body circulatory system to transfer anti-carcinogenic drug to the defected area. Whereas during its transportation process it damages healthy cells and organs therefore making this technique undesirable[36]. Introduction of targeted drug delivery which have potential to replace harmful chemotherapy technique. The idea is to deliver drugs direct to the tumor area without harming/damaging healthy cells and increasing the amount of drug delivered to the tumor area. In this technique magnetic nano particles coated with drug with the help of functionalization of biocompatible layer helping drug to be encapsulated or attached to the surface. External magnetic field is employed to transport drug to the specific site where tumor and cancerous cells are present and with the help of change in temperature, pH or osmolality the drug is released by these magnetic particles to attack cancerous cells[37]. Upon suitable synthesis process Superparamagnetic iron oxide nanoparticles (SPIONs) can be used as a drug carrying agent. SPIONs should be synthesized in a way that prevents its oxidation and by reticuloendothelial system (RES) performed by liver. Due to smaller size these nanoparticles can easily cross biological blockades. By encapsulation of SPIONs their bioavailability and biocompatibility can be increased[38].

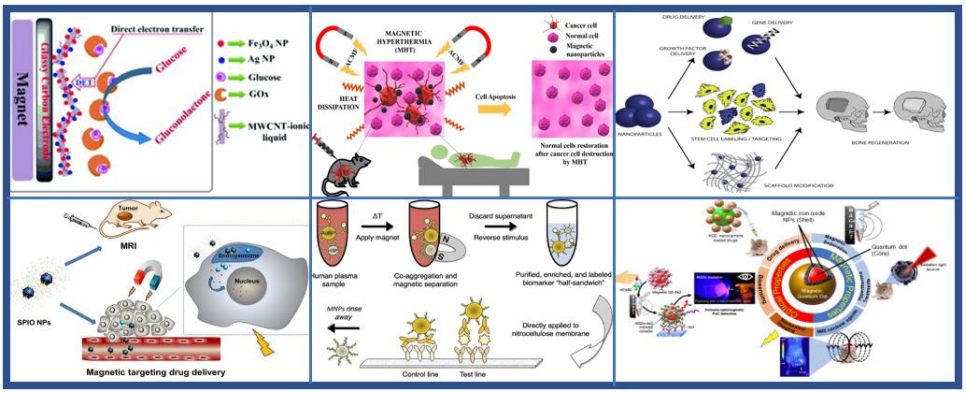

Figure 5: Various Biomedical applications of Iron Oxide Nanoparticles

Hyperthermia is another application in which magnetic nanoparticle can be used. It is a technique in which heat is applied to the area of cancerous cells, as they are highly sensitive to temperature[38]. When the cancerous cells are heated, properties are changed, which will eventually lead to cell death. This treatment is usually used in parallel with chemotherapy and radiotherapy. Hyperthermia is treated locally, regionally and within the whole body. Magnetic nano particle plays an important role in local hyperthermia treatment. Magnetic particles are delivered to tumor areas through direct injection or active targeting in which nano particle are covered with drug related to antibody. Working on the principle of converting electromagnetic energy to heat, these nano particles are distributed around the area where cancerous cells ratio is higher and alternating magnetic field is applied to these localized nanoparticles and heat is generated which helps the magnetic moment in the particle to overcome energy barrier associated with reorientation resulting in energy dissipation which further will result in heat generation via Brownian motion[39]. When polymer coated SPIONs are injected into the body and subjected to alternating magnetic field the domains of SPIONs align themselves in the direction of magnetic field hence generating heat which eventually are able to kill cancerous cell as they are sensitive to temperature. It also helps in inducing apoptosis in tumor cells when loaded with anticancer drug[37].

Different non-invasive bioimaging techniques are used in current medical field which includes ultrasound, magnetic resonance imaging and positron emission tomography[41]. All these techniques produce high quality images using contrast agents but the present contrasting agents have issues regarding toxicity, low imaging and retention time. Many nano particles have shown potential to be upcoming contrasting agents due to their desirable properties like increased biocompatibility and higher

retention time Water molecules are the major components of human body containing two protons. These water molecules contain two hydrogen protons. When the nuclei of these protons are exposed to a magnetic field the spin of each proton align with respect to magnetic field hence aiding in contrast generation which will result in the visibility of internal organs[42]. Super Paramagnetic Iron oxide nanoparticle (SPIONS) have various applications in the field of bioimaging. These nanoparticles are used as an MRI contrast agent. Super Paramagnetic Iron oxide nanoparticles (SPIONs) having size below 5 nm are able to track stem cells[43]. Images of organs are possible to attain by the help of SPIONs. Imaging of cancer cells in conjugation of X-ray imaging were obtained by Sruthi et al[43] .It has been observed that imaging through magnetic particles are superior than MRI alone as more accurate cell's localization is achieved[44].

Photothermal therapy is a technique which uses photosensitiser compound which are non-toxic in nature. But when light fall on these compounds of certain wavelength these compounds become toxic and are used to kill cancerous cells. These types of compounds are usually known as photosensitiser. In this process photo induced electron hole pair are generated which further reacts with molecules like hydroxyl or water molecules forming oxidative radicals leading to cell death[45]. SPIONs can be a potential candidate for these applications.

Superparamagnetic Iron Oxide nano particles (SPIONs) under size of 10 nano meter can be used for separating bio molecule like DNA, Protein and antibodies[49]. SPIONs act as a binding buffer when dispersed in Polyethylene glycol (PEG)[50]. Hydrogen bonding, electrostatic interactions and hydrophobic interactions are the major interaction forces between SPOINs and DNA. The phosphate bond is formed with SPIONs by DNA which can easily be removed by applying a magnetic field and then can be easily recovered by appropriate elusion buffer[48]. Nano core shell SPIONs and Gold nano particles in size of 10 nm can also be used for separation of immune components[47].

Nano particles linked with protein can be used for the function of tissue re-engineering. The SPOINs linked with protein are placed within the damaged tissues and heated above 50^0 C which results in joining of tissues[51]. SPOINS with coating of gold nanoparticles can also be used for tissue repairing by aiding in heat generation by absorption of light. SPIONs in combination of stem cells can be used in field of site-specific repairing as SPOINs can track locate and localized the stem cells at damage tissue site. SPIONS

magnetize the stem cells which aids in retention of these stem cells in the place of damage tissues for tissue re-engineering purposes[52].

1.6 Strontium Based Nanoparticles & Its Applications:

Strontium and strontium coupled nanoparticles are becoming famous from last few years due to its application in the field of biomedicine such as bone engineering, Bioimaging, dentistry, cancer treatment and for efficient drug delivery applications. Strontium, belonging to family of trace metals family, shows similar properties like magnesium and calcium. Strontium is a alkaline earth metal, non-hazardous in nature, is soft silvery white color having atomic number of 38. Earth crust only contains about 0.03% of strontium in a form of carbonates and sulfates. As stated above that strontium acts as calcium and magnesium so human body differentiates between two constructed on human body functions which includes renal uptake, mammary discharge or gastrointestinal (stomach and intestine) absorption.

1.7 Drug Delivery:

Drug delivery is defined as the delivery of healing drugs to the specific site of tumor. It helps in treating diseases like cancer, heart related viruses and unwanted microbes. Conventional techniques like chemotherapy, radiations and surgery are less effective and may have many undesirable effects due to which we are encountering rising trend in cancer cases in both developed and under- developed countries. The various reasons for their little effectiveness include the fact that chemotherapeutic drugs fail to achieve desired levels at the targeted sites due to immunological responses leading to elimination of that drug through excretory system and inability of the surgical procedures to completely eradicate the cancer cells from the body. Due to which the drug injected would not be able to reach target site to completely eradicate the tumor. These drugs are also harmful to healthy cells within the body. Whereas drug delivery offers advantage of target specific delivery with minimal side effects. Magnetic nanoparticles are widely used for this application as these nanoparticles have superior properties like superparamagnetic nature, biocompatible and nontoxic nature[53]. These particles can be guided within the body through external magnetic field. The whole process includes drug loading in which drug is loaded on the nanoparticles and is injected into the body.

Then comes targeted delivery, in which through the help of external magnetic field, the drug is transported to the tumor site and is released through different mechanism like change in temperature, pH and osmolality. Lastly the nanoparticles are removed from the body with the help of kidney, spleen and liver. The delivery of drug to specific site can also controlled by imaging techniques like MRI[54].

Idea of targeted drug delivery was introduced in 1970's[55]. Drug delivery is further categorized in two forms known as active targeting and passive targeting. Passive targeting is based on the mechanism of increasing drug concentration at the site of tumor by the help of permeation and retention effect and also due to the physiochemical properties of nanoparticle which includes size and surface properties. This process offers advantage of high retention of drugs at the tumor site hence increasing the effectiveness of the drug. Despite having advantages this form of targeting have the limitation of poor reliability as it is less controlled mechanism. Whereas active targeting offers advantage of controlled manner delivery of drug as this process is controlled by external magnetics field which helps guiding the particles to the target site and also improves stabilization of nanoparticles at tumor site[57]. Ligands functionalization of MNPs allows further stabilization and accumulation at the tumor site. When drug loaded nanoparticles enter the body through veins their surface is attached by plasma protein on the hydrophobic points and gets recognized by body immune system and thus excreted out of the body[54]. Therefore, in order to retain these nanoparticles within the body surface functionalization of these nanoparticle can be done by hydrophilic compounds like polyethylene glycol (PEG) to make these nanoparticles more biocompatible and more water soluble. Effective treatment by the help of nanoparticle depend upon various factors including nanoparticles concentration, movement time and blood movement rate, biocompatibility of nanoparticles, external magnetic field strength, size and shape of nanoparticles, magnetic properties of nanoparticles, distance and depth to travel by nanoparticles to tumor site and blood flow rate. The drug loaded magnetic nanoparticles are injected into the veins in the form of colloidal suspension and then delivered to the tumor site through external magnetic field[59]. Targeted drug delivery offers advantage of efficient use of drugs, proper target identification and only releasing drug to effected sites

1.8 Research Gap:

As we know strontium and iron oxide nanoparticle have various applications in the field of biomedical science especially in the field of drug delivery as stated above. Their combined effect in the field drug delivery haven't been explored yet or little data is available in scientific research. Effect of strontium addition to iron oxide (doping) properties like drug loading, drug release and cytotoxic behavior haven't been investigated yet. Effect Ibuprofen loaded on this doped material is also being investigated for the first time this research.

1.9 Research Objectives:

This research majorly focuses on the synthesis of Strontium doped iron oxide nanoparticles for drug delivery applications. By taking advantage of biological and magnetic properties of iron oxide nanoparticles incorporating drugs on theses nanoparticles are proven to be efficient way in improving therapeutic effect of these drugs. Iron oxide nanoparticles can actively target to the tumor site with the help of external magnetic field. These nanoparticles properties are governed by their size and shape as for biomedical application size below 100 nm is desired and narrow size distribution is preferred. To ensure good stability and dispersibility in biological environment choice of coating must be selective and efficient as these coating can be modified so that drug release becomes more responsive and any change in temperature, pH or Osmolality.

On the other hand, strontium belonging to group 2 elements having similar properties like calcium and magnesium which is used in various biomedical application due to its nontoxic and biocompatible nature. Strontium can be used in biomedical applications like use as an antimicrobial agent, use in drug delivery application, bone regeneration, waste water treatment, diabetes management, cavity filler, adsorbent and growth promoter. In resent development, strontium has been studied for drug delivery application with porous silica nanoparticles and it can be seen that it has enhance the drug carrier capabilities and has regulated (slowing the rate of release) the drug release capabilities of silica nano particles. Strontium carbonate was also studied showing more

potential antitumor activity than free drug alone. It also showed that strontium nanoparticles were nontoxic to normal cell.

Therefore, doping of iron oxide nano particles with strontium of different content is to be studied in this research and the aim is to study the combine effect of strontium and iron oxide nanoparticles for drug carrying capabilities by doping different amount of strontium in iron Oxide nanoparticles.

1.9.1 Objectives:

The following objectives of this thesis are:

- Synthesis and characterization of strontium doped Iron oxide nano particles via Coprecipitation route.
- Evaluation of drug loading and drug release behavior of Iron oxide (Fe3O4) and Strontium doped Iron oxide nanoparticles (strontium with molar ratio of 0.25,0.5,0.75 & 1)
- Evaluation and comparison of cytotoxicity of these synthesized nanoparticles, both bare and loaded with drug (Ibuprofen).

Chapter 2:

Literature Review

2.1 Iron Oxide Nanoparticles:

Among various types of nanoparticles Magnetite (Fe_3O_4) and Hematite (Fe_2O_3) are most widely used nanoparticulate system due to incredible properties like superparamagnetic nature, biocompatibility, environmentally friendly and stability. One of the ancient ore of iron used by mankind is hematite as a pigment[58]. It has been found that natural hematite can be used in antimicrobial activities when used as a cathode material. Ferrite under the size of 100 nanometer act as superparamagnetic in nature hence can be controlled using external magnetic field[59]. Dispersion is the main focus for these nanoparticles. As in nanoscale particle have higher surface area to volume ratio due to which aggregation and agglomeration occurs. So, to use for various application surface needs to be modified as size and shape plays important role in how nanoparticulate system performs. So, for modification of surface, surface functionalization is used which helps good dispersion of nanoparticles and also helps to connect with another nanoparticle for advance applications[61].

The crystal structure of iron oxide nanoparticle contains oxygen anions and tetrahedral and octahedral sites are occupied by iron cations. In magnetite cubic closed pack structure can be observed showing reflection peaks at (200), (311), (400), (422), (511) and (440). Fe (+3) filled two-third of the crystal structure sites[62][63]. Other ore is hematite in which hexagonal packed structure can be observed having XRD pattern at (012), (104), (110), (113), (024), (116), (214) and (300)[64].

Magnetic material consists of magnetic dipoles that are able to retain magnetization due to alignment of dipoles under the effect of external magnetic field. Whereas superparamagnetic iron oxide nanoparticles show magnetic effect only in the presence of external magnetic field showing no hysteresis after the removal of external magnetic field[66]. The property is a plus for biological applications as they become detectable from external magnetic detectors as they produce heat in the presence of magnetic field. Various ore of Iron behaves differently in the presence of magnetic field and at different temperatures. Talking about hematite its ferrimagnetic at room temperature and at -10 degree centigrade it changes to

antiferromagnetic state. Magnetite at size rang below 20 nm act as super paramagnetic in nature[67] whereas maghemite becomes unstable at higher temperature and show not effect under external magnetic field and at room temperature it is ferrimagnetic in nature.

Ability of nanoparticles to remain monodispersed and resist agglomeration determine their colloidal stability. Iron oxide nanoparticle usually gets degraded and agglomerated due to collision occurring within the particles in the suspension which depends on three major factors including concentration of particles, hydrodynamic flow and Brownian motion generating attractive and repulsive forces[68]. So, the goal is to create an environment in which repulsive forces are higher than attractive forces within the suspension so that particle don't get agglomerated. In order to increase repulsive forces surface functionalization process is used in which outer surface of nanoparticle are covered by polymers including chitosan, Polyethylene glycol, starch and dextran etc. and other organic materials like silica, ascorbic acid and citric acid plays important role in surface functionalization of iron oxide nanoparticle[70]. These coatings are also reducing toxicity, as most of them are biodegradable. Good stability is indicated by zeta potential value above 25mV or below -25mV[71].

Properties of iron oxide nano particles depends upon the size shape and crystallinity of synthesized nanoparticles. These properties are majorly dependent upon the synthesis route and reaction parameters. Iron oxide nanoparticles having size below 20 nanometer[73] plays important role in biomedical applications as below this size range nanoparticles can easily enter tumor site crossing all barriers and creating therapeutic outcomes[75]. The shape and crystallinity also maters as round and crystalline nanoparticles are preferred[76].

Toxicity of nanoparticle is the main barrier to its biomedical application. They get accumulated within the body and become hard to remove[78] as it is found in previous researches that superparamagnetic iron oxide nanoparticles get accumulated within the kidney of rats during experimental trails[79]. So, in order to reduce the toxicity biocompatible and biodegradable coatings are used. Within Iron ore magnetite nanoparticle are found to be less toxic[80].

2.2 Surface Modification of Iron Oxide Nanoparticles:

Iron Oxide nanoparticles are hydrophobic in nature[81]. These nanoparticles contain high surface area to volume ratio due to which agglomeration occurs when particles interact

which each other forming clusters which acts as ferromagnetic in nature and when these clusters interact with each other results in further magnetization of these nanoparticles[82]. Ferro fluids are the magnetics nanoparticles of iron oxide which exist in a form of colloidal solution which is applicable to various biomedical applications. These magnetic nanoparticles suffer from aggregations issue which can be overcome by surface coating or surface functionalization[84]. These surface modifications play's important role in preparing nanoparticles for biomedical applications. surface functionalization also plays important role in enhancing stability and reducing toxicity of nanoparticles. Surface modification can be done by the process of ligand addition method in which material used for surface functionalization like polymers or surfactants are added with the precursors of nanoparticles which get attached to nanoparticles produced by electrostatic or hydrophobic interactions and prevents agglomeration[83]. Second method of modification surface includes the process of ligand exchange in which the original particles surface is changed by functional groups like amine, carboxylic acids, Thiols, Diols etc. The surface of nanoparticles is functionalized according to specific drug nature and the tissue to be targeted. So, the modification of nanoparticles is done through the process of polymer surface exchange or polymer encapsulation process. In Encapsulation method the surface of particles is exchange by the polymer and polymer encapsulation occurs through the process of functionalization in the mechanism of polymer encapsulation process. The polymer used for encapsulation or surface exchange could be of various types which could be synthetic in nature like polyvinylpyrrolidone (PVP), polyethylene glycol (PEG), polyvinyl alcohol and poly lactic coglycolic acid etc[85]. These polymers could be natural in nature like chitosan, starch, gelatin or dextran etc. Chitosan in natural polymers is the most widely studied for biomedical applications due to natural abundance and superior properties like biodegradable, nontoxic, biocompatible and its attractive hydrophilic nature. It is made up of repeated units of hydroxyl and amino group which make it suitable for therapeutic purposes like gene-delivery[86]. The limitation of chitosan of poor solubility can be solved by its derivatization which makes lit glycol chitosan which becomes soluble in acidic and neutral pH environment due to glycol branches[87].

2.3 Iron Oxide Based Drug Delivery:

Iron Oxide nanoparticles are approved by Food and Drug Administration (FDA) for the use for biomedical (in vivo) applications as its ore magnetite and maghemite naturally exist in

human body and are biocompatible in nature. Magnetic Drug Targeting on tumor have recovery rate of about 57% as majority of particles localized on tumor surface. It is better than conventional method as only 1% of the drug is able to reach target site showing extremely low targeting efficiency. Superparamagnetic Iron Oxide nanoparticles (SPIONs) have excellent penetration depth of 10 to 15 centimeter as smaller crystallite size allows them sufficient thermal energy to oscillate in the direction of magnetic field.

Cancer is caused by uncontrolled division of abnormal cells that spreads throughout the body damaging organs and healthy tissues. It is one of the leading causes of death all around the world. Chemotherapy, radiations and surgery are the traditional treatments used to cure this disease which are less effective, noncurative, time limited and lacks specificity having potential to cause severe damages to healthy cells.

The commonly used drugs for the cure of cancer includes Doxorubicin (DOX), Docetaxel (Dtxl), Cisplatin, Bortezomib, Gemcitabine (GEM), Artemisinin and Paclitaxel (PTX). DOX intercalates into the cell DNA and inhibits the DNA replication by inhibiting topoisomerase II[88]. Dtxl inhibits the cell growth by disruption of microtubules dynamics[95]. Cisplatin induces cell damages by crosslinking with the DNA purine bases. Bortezomib inhibit the cell growth by inhibiting protein complexes known as proteasomes which degrade proteins[92]. Gemcitabine impedes DNA long chains which results in cell death[92]. Artemisinin produces free radicals which causes cell damages and slowing the division of tumor cells[91]. PTX disrupts the normal tubule dynamics required for cell division[87].

Magnetic resonance imaging (MRI) assessed targeted drug delivery with the help of iron oxide nanoparticles are extensively studied as they can also be used as a contrast agent with effective drug loading properties. Therefore, Iron Oxide nanoparticles aids in monitoring tumor sites and the treatment against them.

Oleate coated iron oxide nanoparticles synthesized by pyrolysis method of 15 nm size were synthesized by **Xie Et al.** [96]. and were studied by labeling them with 64Cu-DOTA and Cy5.5 which shows prolonged circulation and accumulation at tumor site. Further these nanoparticles were encapsulated with doxorubicin along with dopamine in human serum albumin for tumor targeting having hydrodynamic diameter of around 50 nm termed as ‘D-HINPS. These encapsulated nanoparticles were studied on murine breast cancer model in which it was proved that these nanoparticles have higher tumor clampdown and higher

accumulation effect with respect to doxorubicin and doxil alone. In another in-vitro study these nanoparticles showed better drug loading capabilities due to polyamine coating promoting better cellular uptake[97].

Folic acid conjugated iron oxide nanoparticles were synthesized for the treatment and diagnosis of breast cancer by **Huang Et al.** [97]. The efficacy of these nanoparticles was tested by loading them with Dox and were tested on nude mice having MCF breast cancer tumor. The accumulation of these nanoparticles was tested using MRI as iron oxide nanoparticle have higher R2 relaxivity [98]. Iron oxide nanoparticles coated with heparin loaded with Dox was studied for combined drug delivery and MRI applications. The synthesized system showed better drug uptake efficiency, less cardiotoxic effect and slower drug release rate with respect to Dox alone [100].

Magnetically guided iron oxide nanoparticles have high application in biomedical applications especially in therapeutics applications like drug delivery. External magnetic field is used to guide the nanoparticles to tumor site and also aids in accumulation of these nanoparticles at tumor site [101]. The saturation magnetization of these nanoparticle plays an important role in these applications as higher the saturation magnetization higher will be the control on the path of nanoparticles.

Iron oxide nanoparticles were synthesized via coprecipitation method by **Wagstaff Et al.** group [101]**.** These nanoparticles were coated with using the process of "iterative hydroxylamine seeding" method. With the Help of polyethylene glycol linker, the cisplatin was loaded on these nanoparticles. The synthesized nanoparticles showed 110-fold increase in cytotoxicity on cancer cell line of human ovarian and inhibition of cell growth when attracted by bare magnet.

Iron Oxide nanoparticles were synthesized by **Unterweger Et al.** [102]. These nanoparticles were coated hyaluronic acid which allowed improved drug loading of cisplatin and also enhanced targeting of CD44 receptors in cancerous cells. Formation of polymer metal complex with hyaluronic acid, loading of cisplatin was achieved. The encapsulation efficiency of these drugs was calculated to be around 43.2%. The drug release mechanism was highlighted as burst release on first 30 minutes and after that continuous release for 48 hours indicated as surface bonded drug. An increased drug release was observed which make these nanoparticulate system suitable for target drug delivery applications. The path of these nanoparticles was controlled by neodymium magnet.

Iron oxide nanoparticles coated with Poly Vinyl Alcohol (PVA) and loaded with Dox was studied by **Nadeem Et al.** [103]. Magnetic properties were studied. The control of the path of these nanocarriers were studied through external magnetic field. These nanoparticles showed good control for guided delivery applications of drugs.

Zaloga Et al., [104] synthesized iron oxide nanoparticles coated with human serum albumin (HSA) and lauric acid, having mean diameter of about 7 nanometer and having mitoxantrone adsorbed on the surface of HSA, showed enhanced stability and a linear drug release pattern for approximately 72 hours. These synthesized nanoparticulate system showed potential for site specific targeting in in-vitro systems.

Chitosan coated iron oxide nanoparticles were synthesized by **Natesan and co-workers** [105]. In this study artemisinin was used as an anticancer drug. Chitosan provides added advantage of excellent encapsulation of drugs. Iron oxide nanoparticles with size around 10 nanometers were synthesized by Natesan et al [105]. The drug (chitosan and artemisinin) was loaded on the sample by ion gelation method. Both in-vitro and in-vivo magnetic assisted targeting was examined in glass container and in mice model. The results showed higher drug accumulation in tumor.

Iron oxide nanoparticle coated with polymerized β-cyclodextrin was studied by **Jeon Et al.** [108]. These nanoparticles were loaded with polymerized paclitaxel by inter-particles interactions. High magnetic saturation was observed showing enhance anticancer activities.

Therapeutic specificity of a drug is determined by interactions between antigens and antibodies which allows them to specifically target the disease site. Iron oxide nanoparticles are functionalized with targeting agents like peptides or antibodies which aids in site specific delivery of therapeutic agent. Vectorized nanoparticles are the major focus of many research groups and there testing as targeting agent has been ongoing pursuit.

Iron oxide nanoparticles loaded with gemcitabine (GEM) and further modified with amino-terminal fragment (ATF) peptides were synthesized by **Lee Et al.** [109]. The system was tested on pancreatic cancer tissues which showed increased drug uptake on tumor sites. Peptide linker used due to enzyme sensitive properties helped in controlled drug release by making cleavages through enzymes in cancer cell's intracellular components. Therapeutic and diagnostic application of this system was observed using MRI technique.

Peptide and carboxymethylated-β-cyclodextrin loaded iron oxide nanoparticles were synthesized by **Mu Et al.** [110]. Nanoparticle with size range of about 30 nanometers were used in this nanoparticulate system and were tested on breast cancer cells. The drug used for this study was paclitaxel and the system along with this drug was tested under in-vitro conditions which showed their abilities to target cancer cells.

Two peptides luteinizing hormone-releasing hormone receptor (LHRHR) and Urokinase-type plasminogen activator receptor (uPAR) were conjugated on iron oxide nanoparticles by **Ahmed Et al.** [111]. these nanoparticulate system was termed as 'double-receptor-targeting nanocarriers'. These nanoparticles were tested for treatment and diagnosis of prostate cancer. Both peptides were attached to nanoparticles by formation of amide bonds. These nanoparticles demonstrated good properties like high drug loading, smaller hydrodynamic diameter and negative zeta potential value. These nanoparticles, loaded with paclitaxel, showed increase in cancer cell cytotoxicity and reduction in amount of drug needed to have desired results with respect to concentration needed for free drug only. Other vectorizing agents includes aptamers and antibodies that are being used for drug delivery application.

Iron oxide nanoparticles with average inorganic diameter of about 8 nanometers were synthesized by **Nagesh Et al.** [112]. These nanoparticles were coated with β-cyclodextrin (drug incorporated in its hydrophobic cavity) and pluronic F127 polymer. Docetaxel was loaded on these nanoparticles which showed higher penetration into pancreatic cancer cell due to its desired smaller size. The results showed that this nanoparticulate system is preferable for targeting prostate cancer.

To target prostate cancer cells, nanocarriers targeting prostate specific membrane antigen (PSMA) were developed by **Leach Et al.** [113]. In this research nanoparticle were coupled with biotin-streptavidin for nanoparticles functionalization and loading it with Dox. Dox was loaded by intercalating into double helix of aptamer which are able to identify extracellular areas of PSMA. This system allowed reduction in nonspecific uptake hence reduced untargeted toxicity.

Iron oxide nanoparticles coated with gemcitabine and anti CD44 antibodies were synthesized by **Aires Et al.** [114]. These coatings are capable of targeting CD44-positive pancreatic cancer cells and induces cell death. Iron oxide nanoparticle were functionalized using di-sulfide bonds helping in releasing drug under high reducing environment. The

nanoparticulate system showed selectivity towards cancer cells and fast release under reducing conditions.

Use of functional groups or stimuli-sensitive coating allows controlled drug release at specific sites. Variation of pH between healthy and cancerous cells can be exploited for targeting applications. Cancers cells have lower extracellular pH with respect to healthier surrounding cells [115]. So, this pH difference can be exploited using coating, bonding of nanoparticles sensitive to pH such as liposomes or polymers. Using temperature sensitive coating on iron oxide nanoparticle can play important role in hyperthermia applications and controlled drug release. Iron oxide nanoparticles with acidic environment sensitive functional groups have been worked on by researchers in past decade.

Iron oxide nanoparticles were coated by polyethylene glycol (amine terminated) and then loaded with Dox by covalent bonding via hydrazine linkages sensitive to pH **by Kievit Et al.** [116]. This nanoparticulate system is synthesized to overcome drug resistance encountered in drug-resistant cancers. The synthesized nanoparticle had hydrodynamic diameter below 100 nanometers and negative zeta potential value favoring penetration of drugs into the tumor site. The system showed better drug release in acidic environment. This nanoparticulate system was efficient against multi drug resistance (MDR) with respect to free drug alone hence showing enhance therapeutic effect.

Ph-dependent drug release of nanoparticulated system based on iron oxide nanoparticles was studied by **Gautier Et al.** [117]. In these Dox loaded iron oxide nanoparticle formation of Dox-Fe^{+2} complex was evaluated which binds to hydroxyl groups and dissociates in acidic environment. The system was tested at pH value 4, showing potential toward therapeutic applications as drug release rate was substantially increased. Chitosan, biocompatible in nature, having antitumor properties, shows enhanced solubility in dilute acidic environment which makes its attractive for pH dependent drug delivery application [118].

Magnetic nanoparticles coated with chitosan was studied for pH-responsive therapeutic applications by **Unsoy Et al.** [119]. Having core size of about 6 nanometer, iron oxide nanoparticles were synthesized by coprecipitation method and were coated with chitosan by ionic crosslinking of tripolyphosphate (TTP). The system showed high drug release at pH value 4.2. Same results were observed in another study in which iron oxide nanoparticles were coated by chitosan [120]. Increase in cytotoxicity of these nanoparticles were observed

that free drug alone. More accumulation of nanoparticles was observed around the nucleus than free drug alone.

Iron oxide nanoparticles with chitosan coating and glutaraldehyde linker that is sensitive to pH for drug delivery of doxorubicin was reported by **Adimoolam Et al.** [121]. Due to formation of amide bonds the system became pH sensitive at lower pH values (acidic conditions). The system was found to be effective for delivery of doxorubicin for human breast cancer and ovarian cancer cell lines. Nanoparticle with temperature sensitive coatings of polymers shows enhanced drug release under alternating magnetic field.

Chitosan coated iron oxide nanoparticles, mesoporous in nature and loaded with doxorubicin, was developed by **Zou Et al.** [122]. The system showed enhanced therapeutic effect under alternating magnetic field.

In another study carried out by **Quinto Et al.,** iron oxide nanoparticles were coated with phospholipid-polyethylene glycol having core size of 14 nanometers [123]. The system showed generation of sufficient heat and release of doxorubicin in a controlled manner. Hence proving its application in combined drug delivery and hyperthermia application.

2.4 Strontium Application in Biomedicine:

As stated above that strontium acts as calcium and magnesium so human body differentiates between two constructed on human body functions which includes renal uptake, mammary discharge or gastrointestinal (stomach and intestine) absorption. Strontium, when given in appropriate amount, can play important role in preventing caries in rats[124]. Reduce in fracture percentage in osteoporotic patients is seen by the addition of strontium ranelate [125]. Significant similarities between calcium and strontium can be seen as strontium is transported by the same carrier in central and tubular cells as used for calcium. Similar to calcium, strontium has the capability of forming divalent cations in biological fluids and have to capability of attaching to protein in serum or plasma. The binding process is similar of that calcium, having similar capacity but weaker in nature[126]. In glucose cells mediated by insulin, Strontium was seen to be effective in cell uptake in the condition that was deprived by calcium and magnesium ions. Strontium can play important role in the development of bones in the absence of calcium. Strontium as Sr^{+2} ions can aid in bone repair and can stay in body for longer durations. It helps in preventing bone degradation by preventing osteoclast activities [127]. Decreasing the Wnt pathway inhibitors and increasing

β-catenin expression, strontium increases the transcription of osteogenic factors and prostaglandin expression[129]. Strontium can play role of calcium during blood clotting and muscular contractions[128]. Bones can be strengthened by inducing Strontium coated halloysite nanotubes forming bones through the process of osteoblast[130]. It is the only trace metal corresponded with bone compression. Despite having various advantages in the field of biomedical science there are some drawbacks that needs to be addressed. High dose of strontium through veins can cause hypocalcemia as ca is secreted through renal secretions[131]. On the other hand, strontium chromate has genotoxic and carcinogenic effects that are undesirable[132].

Applications of strontium nanoparticles in the field of biomedicine includes drug delivery, chemo sensor, bioimaging, dentistry, antimicrobial agents, diabetes treatment and bone regeneration applications. Carboxymethyl cellulose (CMC), a biodegradable and biocompatible polymeric material, is used for encapsulation of strontium nanoparticles which aids in the application of bioimaging. As a trace metal strontium can be used for improving the properties of biomaterials. By addition of strontium, Biological and mechanical properties of material can be improved, more tenacity and durability is attained, better control over degradation rate can be seen and enhanced drug release can be observed [130]. Protein kinase activated by nitrogen; its phosphorylation can be improved by addition of strontium treated mesenchymal stem cells[124]. Stem cells derived by human adipose can be enhance by lower dose of strontium ranelate [133]. Graphene nanocomposite doped by strontium, can be used for synthesizing β-enamino ketones by acetylacetone in a solvent-free system when used as an active catalyst [132]. Scaffolds containing strontium can be used for bone engineering[127].

2.5 Strontium Applications in The Field of Drug Delivery:

Optimum route for delivering drug to target site is a major problem[133]. The absorption and adsorption of drug is highly dependent upon the drug size, the smaller the size the better it gets adsorbed or absorbed [134]. Drug can be injected to the body through different route including oral, through inhalation, through mucous membrane or can be applied directly to the part of tumor. If administered by oral route there is a probability that the drug might be degraded due to pancreatic enzymes [135]. Hydrophobic drugs, due to their low adsorption capacity, have lower bioavailability. Whereas hydrophilic drugs have higher solubility

which results in higher local concentration but are unable to achieve pharmacological reactions as they are unable to cross lipid rich membranes. Having high surface area, high porosity, uniformity and controllable pore size, mesoporous materials are gaining significant interest in the field of biomedical applications [136]. Talking about nanomaterial, nanorods have high applications in the field of biomedicine as they can be used for bone substituents, can be used as an anticancer drug carrier and can be used as antibiotics carrier in in-vivo systems. As stated before, Chitosan due to its biocompatible and mucoadhesive properties is an emerging contender for a drug carrying agent. strontium hydroxyapatite nanorods (mesoporous in nature), coated with chitosan were observed to be efficient for transportation of hydrophobic drugs with no toxic effect [137]. Strontium with silica nanoparticles enhanced its drug loading as well as drug release properties [138]. Ibuprofen was loaded on mesoporous Strontium hydroxyapatite, having self-actuated luminescence, to regulate and monitor the process of drug release[139]. Increase in binding efficiency was observed when Silver oxide nanoparticles were doped with strontium up to 5 % for DNA interactive studies[140]. pH selective drug release study was carried out on biodegradable nano system of strontium carbonate nanoparticles, which showed efficient release of anticancer drug in an acidic environment around tumor [141]. Etoposide loaded strontium carbonate nanoparticulate system showed enhance anticancer potential than free drug alone for target delivery applications [142]. For creating stable and efficient immune system, slow release of antigen is necessary. The response of nanoparticles to antigens can be classified by various methods one of which includes direct delivery of drug to immune system. For prolong delivery of antigen of protein to targeted site[143], porous spheres of strontium doped hydroxyapatite were developed to be used as a matrix for transporting protein antigen[144]. The results showed increase in the efficiency of allergen-specific immunotherapy as the developed nanoparticulate system showed mitigation of allergens to dendritic cells. When the same system was loaded with ovalbumin (an allergen), the system increases the stability and integrity of loaded ovalbumin showing good response in in-vivo systems.

2.6 Ibuprofen for Drug Delivery Application:

Ibuprofen, a nonsteroidal anti-inflammatory drug (NSAID), is a derivative of isobutyl-phenyl-propanoic acid used for treating pain from headaches, kidney stones, osteoarthritis,

dental and postoperative diseases. It is also effective against inflammatory diseases like arthritis [145].

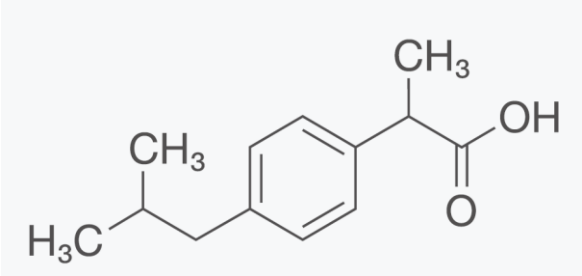

Figure 6: Ibuprofen Chemical formula

In a previous study it has been observed that daily intake of 200mg Ibuprofen reduces the risk of cancer of colon, prostate, breast and lungs by 63%, 39%, 39% and 36%. It has been observed that effect of this NSAID becomes stronger with longer duration and results of these drugs becomes evident after 5 years of use. It is also observed that Ibuprofen has stronger anticancer effects than other NSAIDs like aspirin, especially against breast cancer [146]. In another study it was found that Ibuprofen loaded on nanoparticles showed enhanced anticancer activity on A-549 cancer cell line (lung carcinoma epithelial cells) which was 4-28 time higher than free drug alone[146]. Ibuprofen in conjugation with others anticancer drugs showed enhanced results that are favorable. In a study, Ibuprofen combine effect with cisplatin was observed on lungs cancer cell line. It was observed that the antitumoral activity of cisplatin was improved by addiction of Ibuprofen as Ibuprofen reduces Hsp 70 protein in cancer cells by reducing HSF 1 expression [147]. So, it was evident for the research that Ibuprofen can be used as a potential therapeutic drug that aid in lowering the dose of cisplatin and reducing the challenges of toxicity and drug resistance.

Chapter 3:

Materials & Methods

3.1 Synthesis Techniques:

Synthesis route chosen for making nanoparticles were coprecipitation and hydrothermal techniques. Coprecipitation method is used due to its end product features like will dispersed nanoparticles in water, higher purity is achieved, size can be controlled using surfactant and it's a simple non expensive process of synthesizing nanoparticles. On the other hand, hydrothermal technique is also used for synthesizing nanoparticles for obtaining narrow size distribution of nanoparticles.

3.2 Materials:

Ferric chloride hexahydrate ($FeCl_3.6H_2O$ (99% pure)) was purchased from Merck, ferrous chloride tetrahydrate ($FeCl_2.4H_2O$ (99% pure)) was purchased from sigma Aldrich, Ammonia Solution (32%) was used as a reducing agent, Ibuprofen was used as a sample drug and Deionized water was used for preparation of all solutions.

3.3 Synthesis of Fe_3O_4:

3.3.1 Co-Precipitation:

Iron Oxide nanoparticles (magnetite Fe_3O_4) was synthesized by dissolving 0.2 moles $feCl_3.6H2O$ with0.1 mole of $FeCl_2.4H_2O$ in deionized water. the ratio was kept as 2:1 between Fe^{+3} and Fe^{+2} ions. The mixture was stirred for 1 hours and after that ammonia was added quickly to the solution until pH value reaches to 11. The mixture was stirred at 800 rpm and at 45 °C temperature for 1 hour and after that the black magnetite nanoparticles were magnetically separated and washed several times with ethanol and deionized water. After that the nanoparticles were dried at 60°C in oven for 12 hours and then the dried powder was further grinded to obtain fine powder.

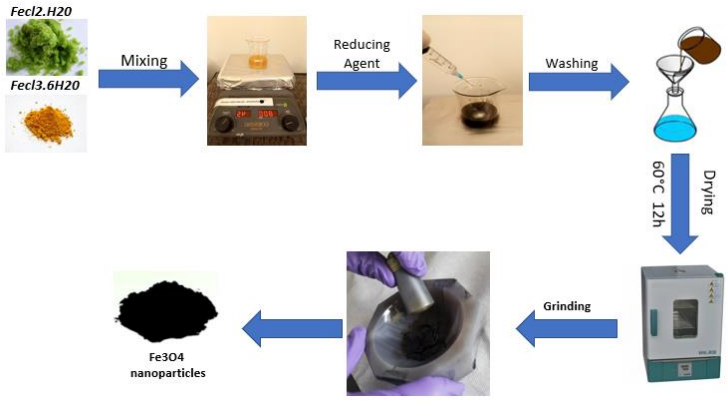

Figure 7: Synthesis route for preparing Fe_3O_4 nanoparticles via coprecipitation technique

3.3.2 Hydrothermal:

Magnetite nanoparticles were synthesized by mixing and dissolving 0.2 moles $feCl_3.6H_2O$ with 0.1 mole of $FeCl_2.4H_2O$ in deionized water. The mixture was stirred at 800 rpm and at 45°C. after 30 minutes ammonia (32%) was added quickly until the pH reached 11. The solution was stirred for 30 minutes and then transferred to Teflon lined 100 ml autoclaved and heated at 134°C for 3 hours. After 3 hours the nanoparticles were magnetically separated and washed with deionized water and ethanol several times. Then the particles were dried for 12 hours in oven. The final product was further grinded to obtain fine powder.

Figure 8: Synthesis route for preparing Fe_3O_4 nanoparticles via Hydrothermal technique

3.4 Synthesis of Strontium Doped Iron Oxide Nanoparticles:

For synthesis of strontium doped Iron Oxide nanoparticles. Strontium was added to initial precursors and was replaced by iron atom (Fe^{+2}). Strontium was added in sequence of 0.25,0.5,0.75 and 1 moles ratio with Fe^{+3} and Fe^{+2} Ions. Synthesis parameters and procedure were same as used for synthesizing iron oxide nanoparticles via coprecipitation and hydrothermal route. Additional step of calcination at 700°C for 4 hours were performed to obtain $SrFe_2O_4$ phase. The molar ratios were calculated using formula:

$$mass\ in\ (g) = \frac{molarity(moles)\ \times molarmass(g/moles) \times (solvent\ taken\ in\ (ml))}{1000\ (ml/l)}$$

Equation 1: Formula For calculating Mass in grams from molar solutions

The calculations of molar ratios used for synthesizing strontium doped iron oxide nanoparticles are given below

SR No.	Fe^{+3} moles	Fe^{+2} moles	Sr^{+2} moles	$FeCl_3.6H_2O$ grams	$FeCl_2.4H_2O$ grams	$SrCl_2.6H_2O$ grams
1	0.2	0.1	0	0.54	0.198	0
2	0.2	0.075	0.025	0.54	0.149	0.066
3	0.2	0.05	0.05	0.54	0.099	0.133
4	0.2	0.025	0.075	0.54	0.049	0.199
5	0.2	0	0.1	0.54	0	0.266

Table 3:Nanoparticles sample Compositions

3.5 Drug loading on Nanoparticles:

Ibuprofen was used as a sample drug to load on these nanoparticles. For loading nanoparticles 15 mg of nanoparticles were added to 10 ml of ethanol solution for each composition. Then 15 mg of Ibuprofen was added to the solution to make the concentration of 1.5mg of drug per ml (1.5mg/ml). Each composition solution was stirred for 24 hours to load the drug. Then the drug loaded sample was separated using centrifugation process at 4000 rpm for 15 minutes. The remaining supernatant was analyzed using UV vis

spectrophotometer absorption spectrum at 264 nanometers to check the amount of unloaded drug.

3.6 Cytotoxicity Testing:

MTT assay is used for determining the cytotoxicity of iron oxide, strontium doped iron oxide and Ibuprofen loaded nanoparticles**.**

3.6.1 Material and Equipment:

Hep-2 cell laryngeal cancer cell line was obtained from National Institute of Health, Iron oxide nanoparticles, strontium doped nanoparticles, and Ibuprofen loaded nanoparticles were synthesized for characterization. Biosafety cabinet, incubator with CO2, 96 well plate, Single channel and multi-channel pipette were used from cell culture lab. Other chemical includes MTT (3-(4,5-dimethylthiazol-2-yl)-2,5-diphenyltetrazolium bromide), dimethyl sulfoxide (DMSO) and Hank's Minimum Essential Medium Liquid (HMEM) which procured in required amount. BIOTEK absorbance microplate reader was used to take absorbance values of each well.

Figure 9: ***Materials and Equipment Used for MTT Assay***

3.6.2 MTT Assay Methodology:

Hep-2 laryngeal cancer cell line was obtained in a form of 10 lac cells per milli liters (ml). to make it 10,000 cells per well 10 microliters(µl) of cell solution was added in each well along with HMEM. These cells were incubated for 24 hours at 35^{o} C with CO_2 content at 5%. Iron Oxide nanoparticles, Strontium doped Iron oxide nanoparticles and Ibuprofen loaded nanoparticles were prepared in different concentration of 300 µg/ml, 400 µg/ml and 500 µg/ml were prepared. The following concentration prepared and their respective addition location in 96 well plate containing Hep-2 cancer cell line are:

Table 4: Samples and their related Symbols for 96-well plate

Samples	***Concentration***	***Symbol***
Fe_3O_4	**300µg/ml**	**1.1**
Fe_3O_4	**400µg/ml**	**1.2**
Fe_3O_4	**500µg/ml**	**1.3**
$Sr_{0.25}Fe_{2.75}O_4$	**300µg/ml**	**2.1**
$Sr_{0.25}Fe_{2.75}O_4$	**400µg/ml**	**2.2**
$Sr_{0.25}Fe_{2.75}O_4$	**500µg/ml**	**2.3**
$Sr_{0.5}Fe_{2.75}O_4$	**300µg/ml**	**3.1**
$Sr_{0.5}Fe_{2.75}O_4$	**400µg/ml**	**3.2**
$Sr_{0.5}Fe_{2.75}O_4$	**500µg/ml**	**3.3**
$Sr_{0.75}Fe_{2.25}O_4$	**300µg/ml**	**4.1**
$Sr_{0.75}Fe_{2.25}O_4$	**400µg/ml**	**4.2**

$Sr_{0.75}Fe_{2.25}O_4$	500µg/ml	4.3
$SrFe_2O_4$	300µg/ml	5.1
$SrFe_2O_4$	400µg/ml	5.2
$SrFe_2O_4$	500µg/ml	5.3
Ibuprofen loaded Fe_3O_4	300µg/ml	B.1
Ibuprofen loaded $Sr_{0.25}Fe_{2.75}O_4$	300µg/ml	B.2
Ibuprofen loaded $Sr_{0.5}Fe_{2.5}O_4$	300µg/ml	B.3
Ibuprofen loaded $Sr_{0.75}Fe_{2.25}O_4$	300µg/ml	B.4
Ibuprofen loaded $SrFe_2O_4$	300µg/ml	B.5
Phosphate Buffer saline (Control)	Varied conc	C

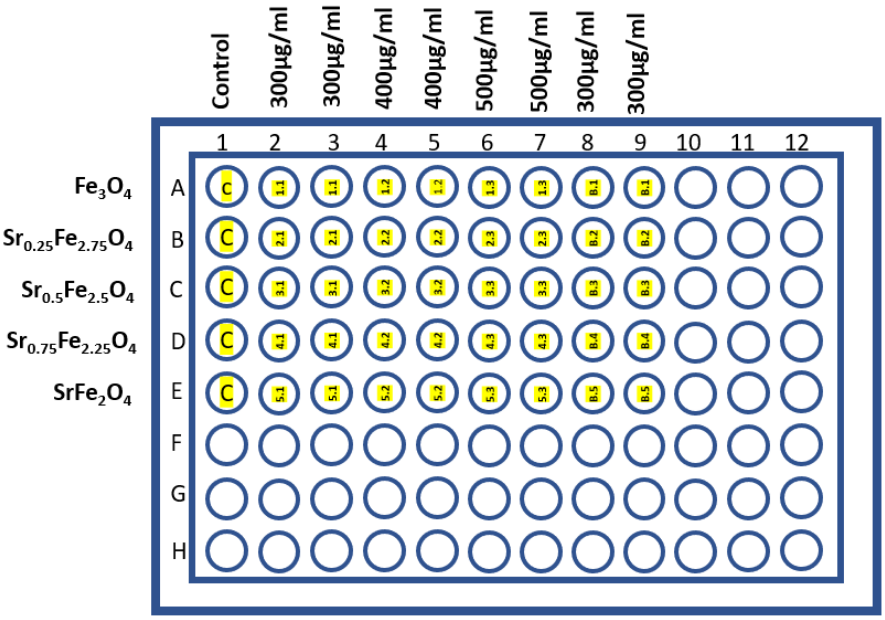

Figure 10: ***Nanoparticles Arrangements in 96-well plate***

Nanoparticles added 96-well plates having cells previously incubated for 24 hours are again incubated at same conditions for 24 hours. Total volume of each well is 200 µl Phosphate buffer saline (PBS) was used as control. MTT solution was prepared in phosphate buffer saline solution having ratio of 5mg/ml. After 24 hours of incubation 20µl of MTT was added in each well and then the 96-well plate was incubated for 4 hours. After that excess solution was removed from each well and to solubilize formazan crystals, 200 µl dimethyl sulfoxide (DMSO) was added in each well and then absorbance reading was taken with the help of BIOTEK absorbance microplate reader at wavelength of 595 nm.

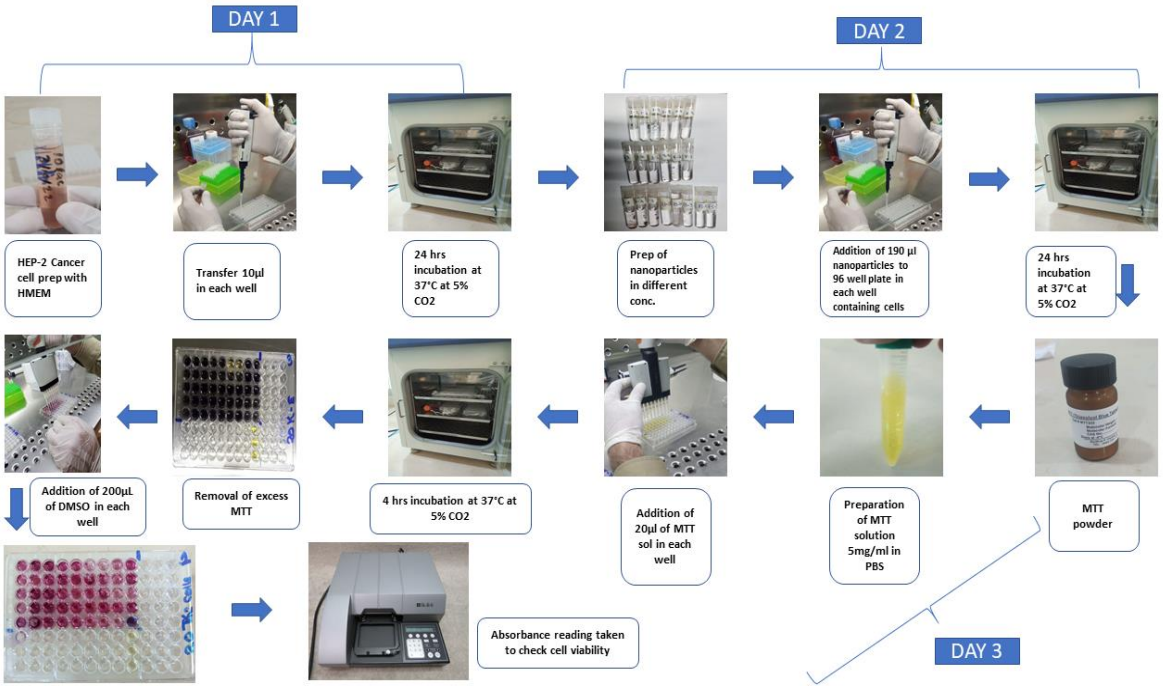

Figure 11: ***MTT methodology followed for cytotoxicity testing of nanoparticles***

Chapter 4:

Characterization Techniques

4.1 X-Ray Diffraction Techniques:

A nondestructive technique used to find out the lattice spacing of crystalline solids which can be used to identify elastic properties residual stresses and identification of unknown material. Lattice spacing is determined when x rays enter the material with known wavelength and angle which passes through atomic planes and gets refracted to diffractometer through which the intensity is measured. X-rays are fired toward the sample at different angles so that planes at different angles can be activated so that proper identification of planes present can be identified. Miller indices (hkl) and atomic spacing of powder sample are usually identified by irradiation these powders through X-rays. The intensity readings obtained corresponds to a specific element or phase. Multiple intensity peaks can be seen in the sample contains multiple elements or phases present.

X-rays are generated by a copper target material when electrons produced from a heated filament bombard the target material which dislodges the inner shell electrons. These produced x-rays are collimated and directed onto the sample from where these X-rays deflects back by satisfying brags law through constructive interference and gets recorded by a diffractometer which converts these signals to counts (peaks) recorded on computer screen.

X-Ray Diffraction is used for identification of crystalline phases present and their respective orientation. It is also used for determination of structural properties like grain size, strain, lattice parameters, atomic arrangement, composition of phase present and measuring thickness of thin films and multi layers material.

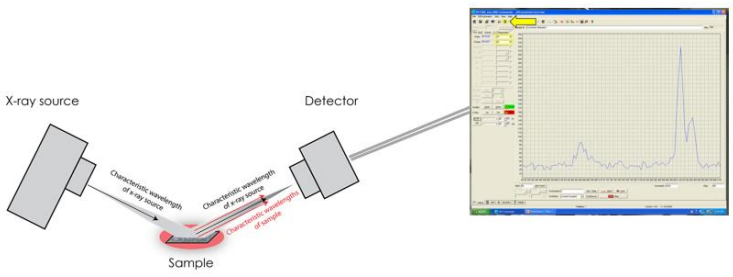

Figure 12: Experimental setup of X ray Diffraction technique

To analyze the nanoparticles through XRD for structure and phase identification, small quantity finely grinded nano powder is taken and was tested through XRD machine available at angle 2 θ, scanning from 0^o to 75^o at step size 0.04 for 50 minutes. The obtained results were compared with reference JCPD file for phase identification. For calculation of crystallite size, Scherrer equation is used.

$$\boldsymbol{Crystallite\ size\ (nm)} = \frac{\boldsymbol{Shape\ Factor(k) \times Xray\ wavelenght\ (\lambda(nm))}}{\boldsymbol{COS\ (\theta(radians)) \times Full\ width\ at\ Half\ Maximum\ (FWHM(radians))}}$$

Equation 2: Debye Scherrer formula for calculating crystallite size

4.2 Scanning Electron Microscopy:

In this techniques variety of signals are generated using high energy electron beams. The information derived by electron sample interaction includes surface morphology, orientation, chemical composition and crystalline structure of the material. Usually a 2-dimensional image is generated showing the surface properties of the samples. Area up to 5 microns can be imaged using scanning electron microscope having resolution from 50 to 100nm in magnification range of 20X to 30000X. Selective analysis can be done through scanning electron microscopy through which we can determine chemical composition using Energy dispersive X-Ray (EDX).

Variety of signals are generated by accelerated electrons interacting with the sample. These signals include secondary electrons (used for determining morphology and topography), backscattered electrons (used for showing contrast in the composition), photons (used for elemental analysis), visible light and heat. SEM is considered to be a “non-destructive” technique as by production of different signals does not cause volume loss hence same sample can be tested again and again.

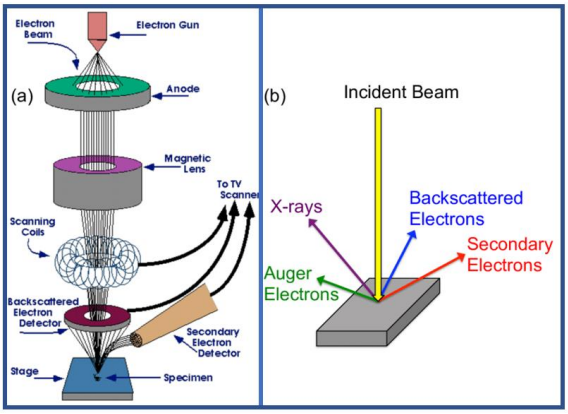

Figure 13: Experiential setup For Scanning electron Microscopy (A), Different rays reflected from Incident beam (B)

To Characterize the nanoparticles, the samples were prepared by sonicating these nanoparticles in deionized water for 1 to 2 hours. After that a drop of the mixture was poured on a glass slide and then dried at 60^{o} C for 1 hour. Then the glass slide was placed on a stub to gold plate it to make the sample conductive and after that the sample was place in low vacuum chamber to characterize the sample using SEM technique. Image were taken at different magnification and resolution using accelerating voltage of 20 kV.

4.3 Fourier-Transform Infrared Spectroscopy (FTIR):

FTIR works on the principle of infrared rays absorbed by the material. The materials ability to absorb infrared light energy at different wavelengths which is used to determine molecular structure and composition. FTIR technique is used for the determination of different types of functional groups present on the surface of sample, which is performed in the range of 4000cm-1 to 400cm-1using infrared rays from spectrometer. Samples are usually prepared by mixing nanoparticles with potassium bromide (KBr) and hen pressing it with the help of uniaxial press into a pellet which is further used for characterization.

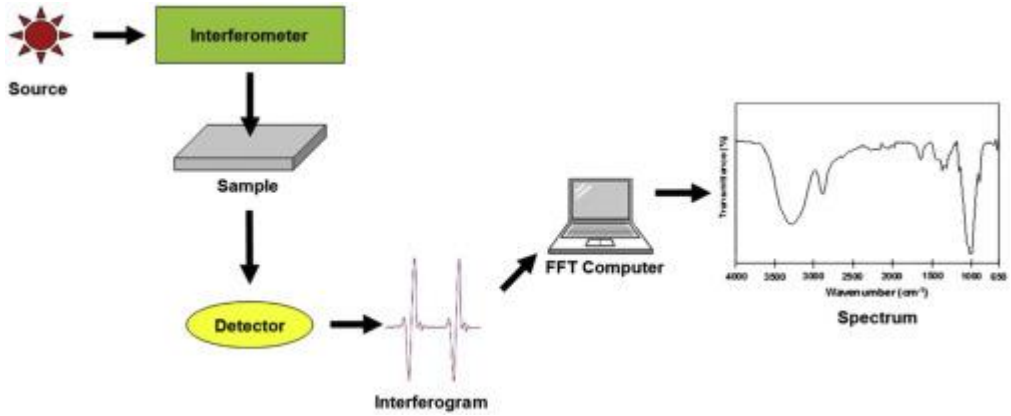

Figure 14: FTIR Setup

4.4 Vibrating Sample Magnetometer (VSM)

In this characterization technique is used to determine the saturation magnetization and magnetic behavior of nanoparticles. The sample is placed in a constant magnetic field and by aligning the magnetic domains of sample, the sample is magnetized. By aligning the magnetic domains magnetic field is generated around the sample which is usually known as magnetic stray field. This magnetic stray field changes when the sample is moved up and down in magnetic field which is detected by pick-up coils which generate an emf in these coils according to faraday's law of induction. The current generated will be proportional to the magnetization o the sample. The greater the induce current the greater will be the magnetization. The signals received by the detector are converted by a software to a graph of magnetization (M (Y-axis)) and magnetic field Strength (H (X-axis) known as a hysteresis loop.

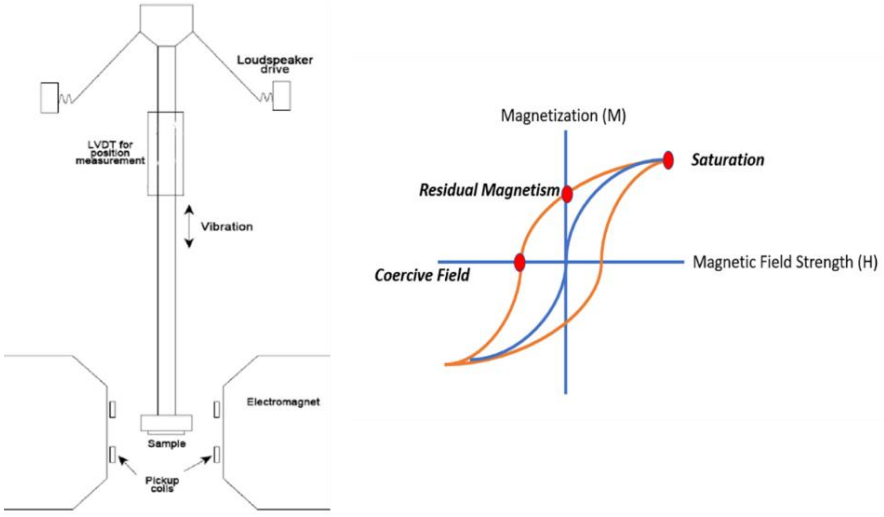

Figure 15: VSM Setup & Hysteresis Curve

4.5 UV-Vis Spectroscopy:

This technique works on the principle of amount of ultraviolet (UV) or visible light absorbed by the sample in comparison to a reference/blank sample providing the information about sample specification (as specific material absorb light at specific wavelength) and its concentration. UV light is usually used for characterizing the sample as UV has wavelengths shorter than visible light hence generating higher energy (frequency). Specific sample has maximum absorbance value at specific wavelength which is used to extract information about the material.

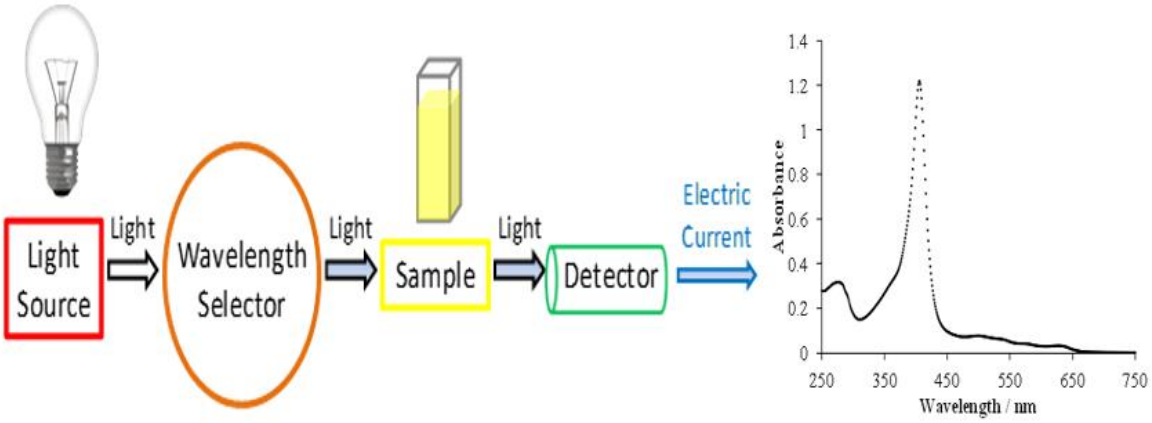

Figure 16: A simplified schematic of the main components in a UV-Vis spectrophotometer

A light source usually of Xenon lamps, a high intensity light source, is used to generate light which is filtered by a monochromator to a desire wavelength and to improve signal to noise ratio which is then passed through a reference sample and from the sample to be tested. Quarts cuvettes are used as sample holders. Initially both reference and main sample cuvettes are filled by the same medium used filling the sample. After one run, one cuvette containing blank is replaced by solution containing sample with the same solvent as used before for characterization. The signals generated are detected by a detector and then displayed on a monitor as a graph between absorbance (Y-axis) and wavelength (X-axis).

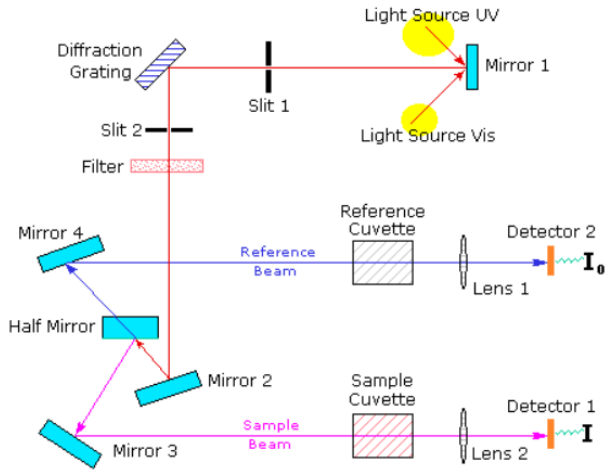

Figure 17: Path that UV light takes to pass through Reference and sample cuvette

The absorbance value identified is equal to light intensity (Io) before passing the sample divided by intensity after passing through the sample (I). The inverse relation of these tow quantities gives us the transmission values. The concentration of the sample in mol L-1 could be determined by using Beer-Lambert's law when quantities like molar absorptivity, path length and absorbance values are known

$$A = \varepsilon\, L\, c = \log_{10}\left(\frac{I_0}{I}\right) = \log_{10}\left(\frac{1}{T}\right) = -\log_{10}(T)$$

Equation 3: relationships between absorbance A, Beer–Lambert's law, light intensities measured and transmittance.

To characterize the nanoparticles all the samples were dissolved in de ionized water with solute to solvent ration of 1mg/1ml. quartz cuvettes were used to filled the sample and characterization range of 200-300 nanometer is used.

4.5.1 Drug Loading and Release Studies:

Drug loading capacity of nanoparticles were determined on calculation based on UV-Vis Spectroscopy at 264 nm wavelength. Ibuprofen is used as a sample drug to load on these nanoparticles. To determine the standard curve of Ibuprofen different dilutions were

prepared using ethanol as solvent containing 0.2mg/ml to 1mg/ml Ibuprofen solution in ethanol. By this linear plot of Ibuprofen was obtained which is further used for calculation amount of drug loaded. For loading nanoparticles 15 mg of nanoparticles were added to 10 ml of ethanol solution for each composition. Then 15 mg of Ibuprofen was added to the solution to make the concentration of 1.5mg of drug per ml (1.5mg/ml). Each composition solution was stirred for 24 hours to load the drug. Then the drug loaded sample was separated using centrifugation process at 4000 rpm for 15 minutes. The remaining supernatant was analyzed using UV vis spectrophotometer absorption spectrum at 264 nanometers to check the amount of unloaded drug. Encapsulation efficiency was determined using following equation.

$$Encapsulation\ Efficiency\ (\%) = \frac{Initial\ Drug\ weight - Free\ drug\ weight\ in\ the\ Spernatant}{Initial\ Drug\ weight}$$

Equation 4 Encapsulation Efficiency Calculations

The amount of drug released was determined by testing drug loaded samples in phosphate buffer saline solution. the drug loaded samples were dispersed in phosphate buffer saline at 37°C temperature under constant stirring. After selected time intervals 3ml of solution is withdrawn and refilled by fresh PBS solution keeping total volume same. The amount of released drug was determined as a function of soaking time via UV-vis spectroscopy at 264nm wavelength. The amount of drug released is evaluated on the basis of following equation.

$$\%\ Drug\ Content = \frac{Amount\ of\ drug\ detected}{Theoretical\ amount\ of\ drug\ used} \times 100$$

Equation 5: Drug Release Calculations

4.6 Cytotoxicity Testing (MTT assay):

Cytotoxicity of nanoparticles is determined using MTT assay. MTT(3-(4,5-dimethylthiazol-2-yl)-2,5-diphenyltetrazolium bromide) assay is a non-radioactive, colorimetric test which is used to measure cytotoxicity, viability of cells and their respective proliferation [148]. This assay is based on the principle of converting yellow MTT salt to purple crystals of formazan via cells activated metabolically. Healthy cells contain Nicotinamide adenine dinucleotide phosphate (NADPH) dependent oxygenase's enzymes which reduces MTT to formazan crystals which are insoluble in nature. These insoluble crystals are dissolved using solubilization agent like dimethyl sulfoxide (DMSO) which result in a colored solution which is measured using multi-well spectrophotometer in wavelength ranges from 500 to 600 nanometers. Number of viable cells is directly proportional to the darkness of the solution in each well. The darker the solution, more viable and active cells are present.

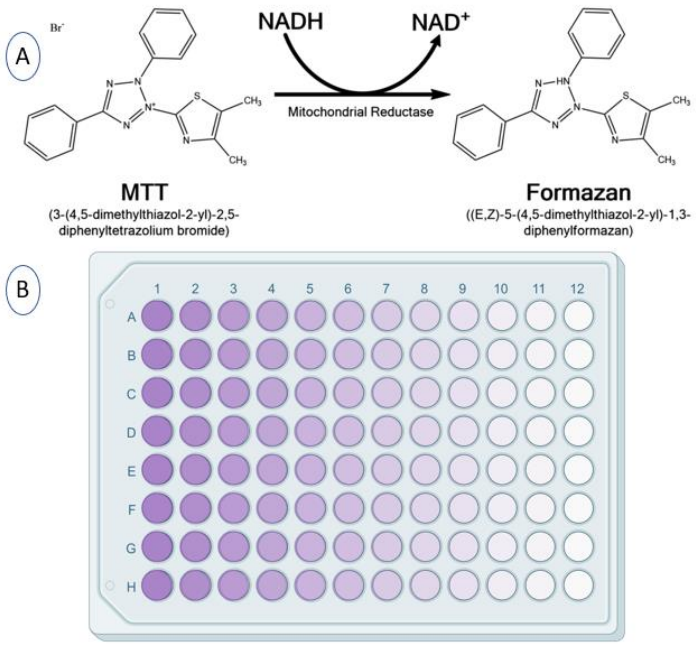

*Figure 18:**Conversion of MTT to a formazan salt by viable cells (A)Formazan crystals in a 96-well plate (B).***

Chapter 5:

Results and Discussions

5.1 X-Ray Diffraction (XRD) Results:

5.1.1 Fe_3O_4:

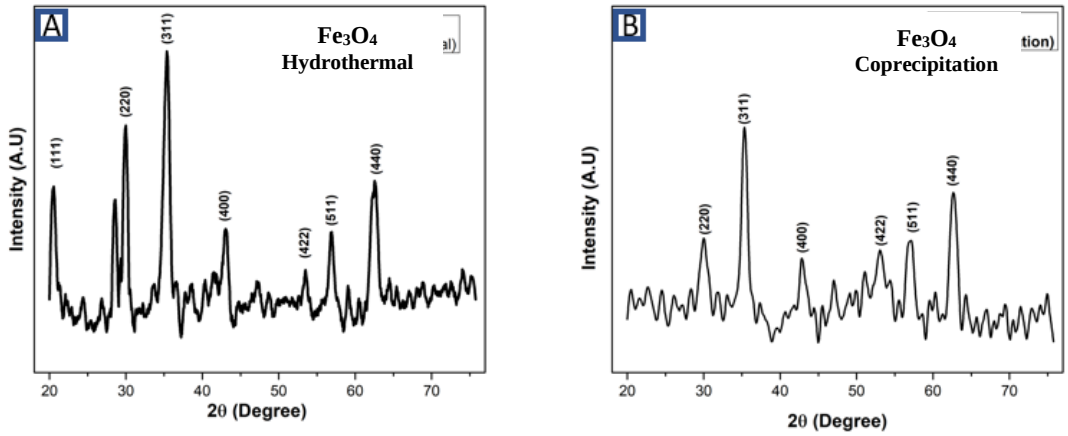

Figure 19: XRD Graph of Fe_3O_4 prepared by Hydrothermal (A) and Coprecipitation (B) method

Patterns of Fe_3O_4 nanoparticles produced by hydrothermal (A) and Coprecipitation (B) has been shown in above graphs. In hydrothermal produced Fe_3O_4 nanoparticles peaks can be observed at 2θ value of 19.9, 30, 35.5, 43.026, 53.6, 56.9 and 62.54. In coprecipitation peaks were observed at 30.04, 35.32, 42.80, 53.08, 57.015 and 62.66. These are in accordance with standard JCPD card [01-088-0315] [149] showing miller indices (2 2 0), (3 1 1), (4 0 0), (4 2 2), (5 1 1) and (4 4 0) at 2 θ value of 30.2°, 35.5°, 43.2°,53.5o, 57.2°,62.7 °. proving the formation of inverse cubic spinal structure of Fe_3O_4. The results in accordance to standard JCPD card shows the formation of black magnetite nano powder. Sharper peaks indicate good crystalline structure have been formed. The broader peaks indicate formation of smaller crystallite sizes which is calculated using Debye–Scherrer formula. Calculated crystallite sizes were:

Table 5: Crystallite sizes of prepared Fe3O4 nanoparticles

Material	Crystallite size (nm)	
	Mean	STDEV
Fe_3O_4 (hydrothermal)	8.3365	2.453
Fe_3O_4 (Coprecipitation)	6.088	1.783

5.1.2 Strontium Doped Iron Oxide Nanoparticles:

5.1.2.1 Hydrothermal:

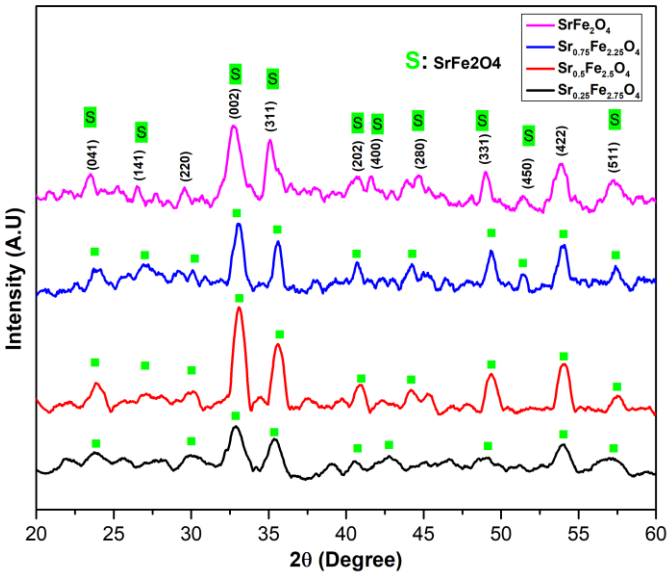

Figure 20: XRD graphs showing strontium doped iron oxide nanoparticles with strontium content 0.25, 0.5, 0.75 and 1 moles

X-ray diffraction peaks of synthesized samples through hydrothermal technique are in accordance to reference code [00-048-0156] showing orthorhombic structure[150] (showing diffraction angles of 2θ of 22.34◦, 24.16◦, 27.71◦, 33.08◦, 35.51◦, 40.89◦, 42.92◦, 45.76◦, 49.38◦, 52.75◦ and 57.62◦ showing Miller indices of (121), (041), (141), (002), (311), (202), (400), (280), (331), (450), and (511)) . Peaks that matches to reference codes includes peaks at 2θ angle 23.872, 27.14, 32.88, 40.62, 42.710, 44.64, 49.37, 52.01 and 57.42 that relates to $SrFe_2O_4$ phase (planes) [151][152]. As the amount of strontium increases from 0.25 molar to 1 molar, the peaks become sharper and more peaks related to $SrFe_2O_4$ phase appears, showing increase in crystallinity and phase purity. Another factor that showed more sharper

peaks is due to increase in crystallite size. Broad peaks indicate smaller crystallite size which is evident from calculation from Debye–Scherrer formula. Extra peaks at 2θ value 30.12 and 54.15 showed the presence of magnetite phase. Peak shift up to 1 degree can observed due to strain induces because of high temperature sintering conditions. The calculated crystallite sizes are

Table 6: Crystallite sizes of prepared Strontium doped nanoparticles with different compositions by Hydrothermal method

Sample	Crystallite Size (nm)	
	Mean	STDEV
$Sr_{0.25}Fe_{2.75}O_4$	6.2078	3.1379
$Sr_{0.5}Fe_{2.5}O_4$	8.1188	2.179
$Sr_{0.75}Fe_{2.25}O_4$	12.283	4.047
$SrFe_2O_4$	12.059	4.7383

5.1.2.2 Coprecipitation:

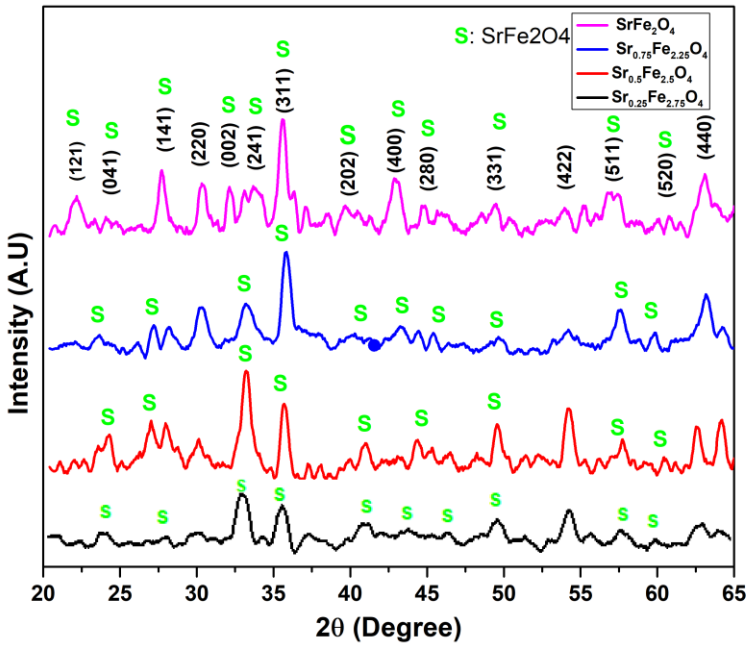

Figure 21: XRD graphs showing strontium doped iron oxide nanoparticles with strontium content 0.25, 0.5, 0.75 and 1 moles

X-ray diffraction peaks of synthesized samples through Coprecipitation technique are in accordance to reference code [00-048-0156][150] showing orthorhombic structure (showing diffraction angles of 2θ of 22.34◦, 24.16◦, 27.71◦, 33.08◦, 33.79◦, 35.51◦, 40.89◦, 42.92◦, 45.76◦, 49.38◦, 52.75◦ and 57.62◦ showing Miller indices of (121), (041), (141), (002),(241) (311), (202), (400), (280), (331), (450), and (511)) [151][152]. As the amount of strontium

increases from 0.25 to 1 molar the phase purity increases and more peaks corresponding to $SrFe_2O_4$ phase appears. At 1 molar peaks at angle 2θ 22.12 and 33.72 corresponding to miller indices (121) and (241) appears. As the amount of strontium increases there can be seen trend of increasing crystallite size as evident from calculated values through Debye–Scherrer formula. As the strontium content increases peak with highest intensity change which is evident from the graph. In sample containing 0.75 and 1 moles of strontium peak having the highest intensity is at 2θ value 35.5◦ which corresponds to spinal structure meaning maximum number of atoms are lying in that plane. Whereas samples containing 0.25 and 0.5 moles of strontium peak with highest peak is at 2θ value 32.89◦ corresponding to (002) plane. Meaning maximum number of atoms are lying in that plane. Peak shift up to 1 degree can observed due to strain induces because of high temperature sintering conditions. The calculated crystallite sizes are**:**

Table 7: Crystallite sizes of prepared Strontium doped nanoparticles with different compositions by Co precipitation method

Sample	Crystallite Size (nm)	
	Mean	STDEV
$Sr_{0.25}Fe_{2.75}O_4$	8.9541	4.6763
$Sr_{0.5}Fe_{2.5}O_4$	11.8	3.4498
$Sr_{0.75}Fe_{2.25}O_4$	10.048	4.4055
$SrFe_2O_4$	12.196	5.133

5.2 Scanning Electron Microscopy:

5.2.1 Fe_3O_4:

Figure shows sample Fe_3O_4 nanoparticles on a glass substrate observed using scanning electron microscope prepared by coprecipitation method. Sample was prepared by dissolving small quantity of nanoparticles in Deionized water and then sonicating these nanoparticles for at least one hour and then placing it on the glass substrate and then gold plated it for making it conductive for further characterization. SEM image shows formation of nanoparticles in nanometer range with majority of particles with spherical morphology[149]. it can be observed from the image that smaller particles aggregated together to form larger particles due to dipole and magnetic interactions. Due to their smaller size (having high specific surface area) and high surface energy, agglomeration can be seen. As no coating was used and these were bare magnetite particles clustering can be observed. The particles show broad size distribution. Image shows majority of nanoparticles below 100 nm which is ideal for biomedical application.

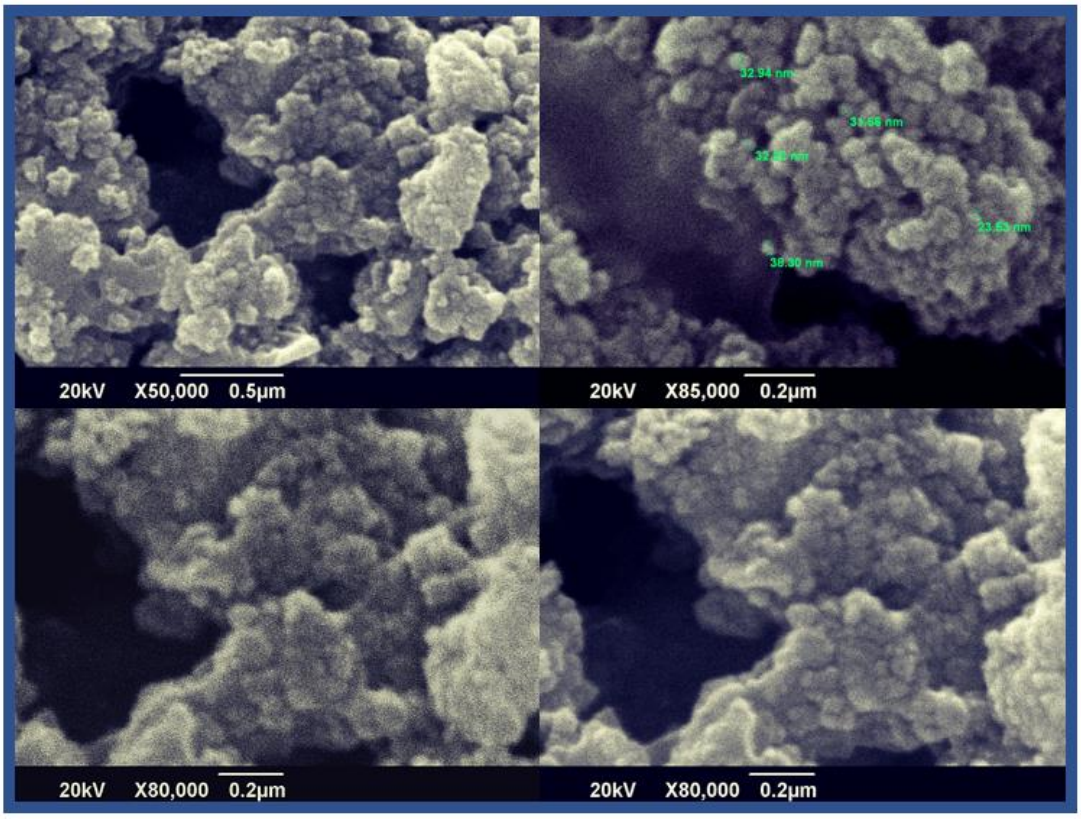

Figure 22: Scanning Electron Microscopy micrographs of Fe_3O_4 nanoparticles

5.2.2 Strontium Doped Iron Oxide Nanoparticles:

Strontium ferrite ($SrFe_2O_{4)}$ nanoparticles prepared by coprecipitation techniques sintered at 700 ◦C can be observed in SEM images from figure given below. Aggregation of particles can be seen due to fine size of nanoparticles and due to fine size, the surface energy increases due to which particles tends to agglomerate and forms larger secondary particles as evident from the SEM images. The major reason for large aggregation is due to combustion process (sintering of particles at 700◦C for 4 hours) which causes interfusion of nanoparticles through chemical reaction. Majority of nanoparticles have spherical morphology having size below 100 nanometers with moderated size distribution. Similar results can be observed in previous research works [153][154].

5.2.2.1 $Sr_{0.25}Fe_{2.75}O_4$:

As strontium is added to Iron oxide nanoparticles, we can observe increase in particle size and the ratio of spherical particles decreases. Particles are agglomerated due to no use of surface coating agent. Majority of nanoparticles can be seen in size range of 30nm to 40nm.

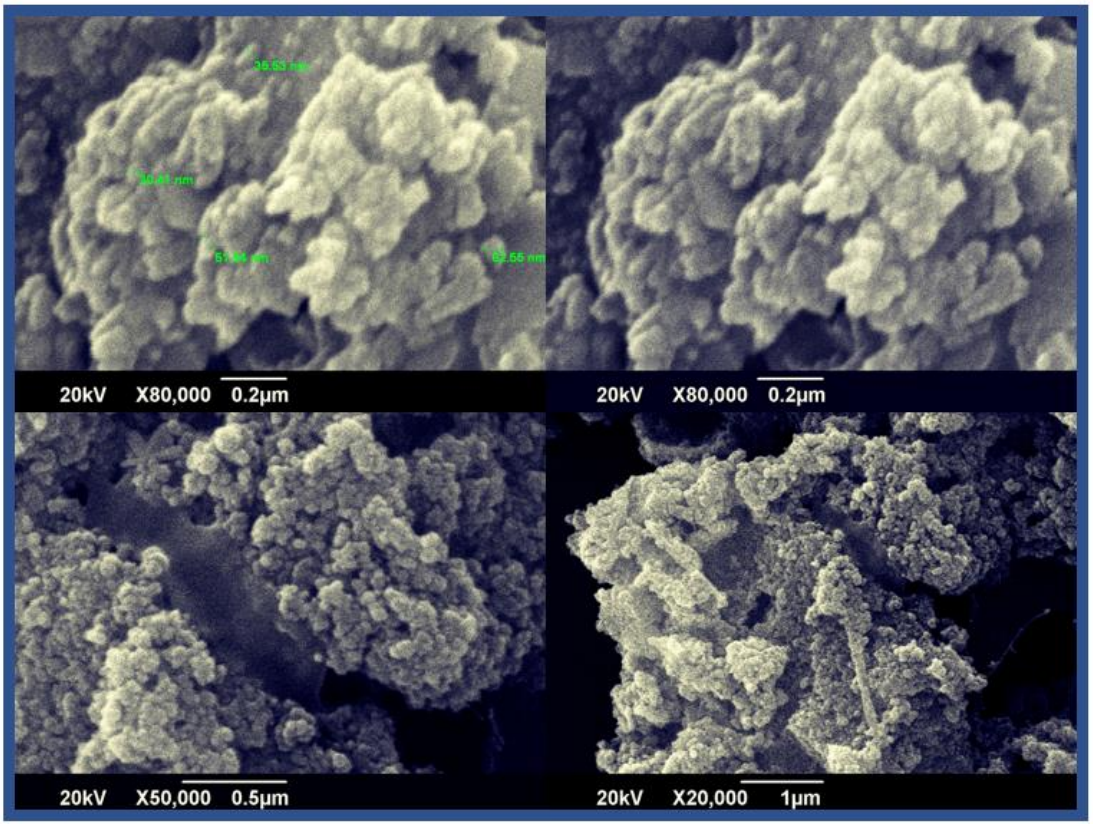

Figure 23: Scanning Electron Microscopy micrographs of$Sr_{0.25}$ $Fe_{2.75}O_4$ nanoparticles

5.2.2.2 $Sr_{0.5}Fe_{2.5}O_4$:

On further addition of strontium, we can see increase in particle size. The particles are mostly in spherical morphology and agglomeration and aggregation of particles can be seen due to high surface area (high surface energy) and lack of use of surface coating agent.

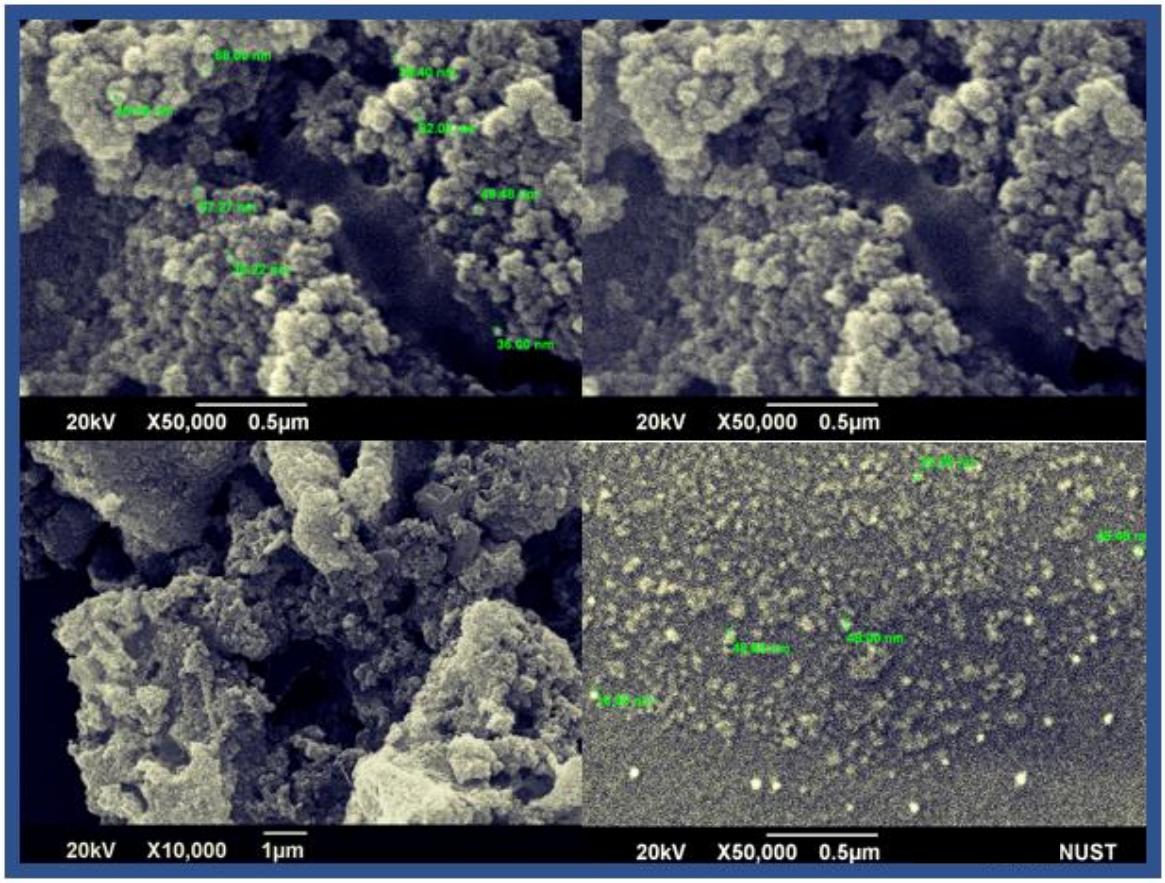

Figure 24: Scanning Electron Microscopy micrographs of$Sr_{0.5}$ $Fe_{2.5}O_4$ nanoparticles

5.2.2.3 $Sr_{0.75}Fe_{2.25}O_4$:

With the increase of strontium to 0.75 mole we can observe further increase in particle size. As the majority of particle size now lies between 50-80 nanometers. Spherical morphology can be observed but some particles with wire shape morphology can be observed. Particles aggregation is due to high surface energy.

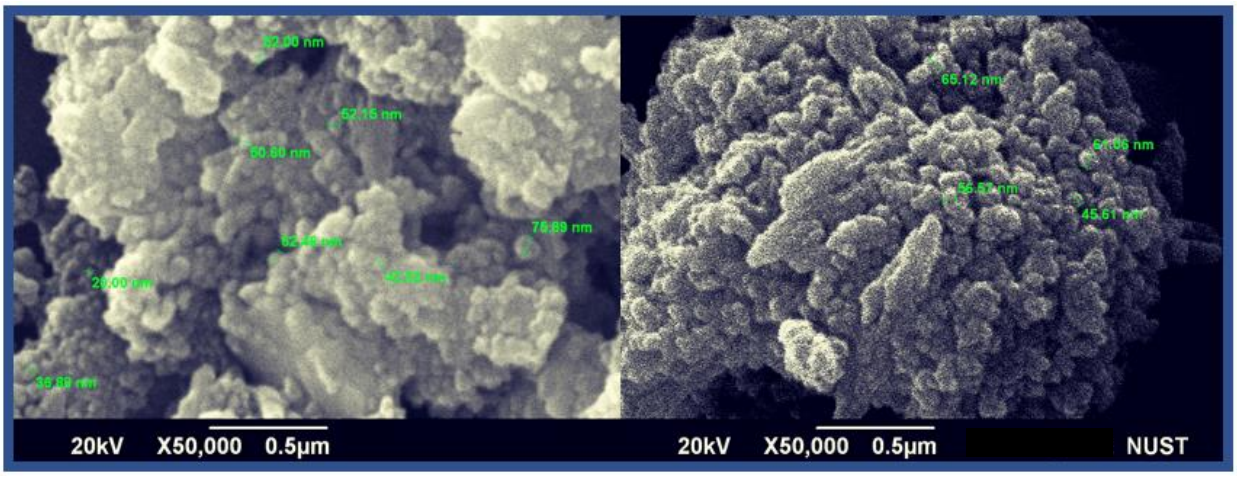

Figure 25: Scanning Electron Microscopy micrographs ofSr0.75 Fe2.25O4 nanoparticles

5.2.2.4 $SrFe_2O_4$:

With strontium content up to 1 molar we can observe more particles with wire shape morphology which is also observed in previous researches. Increase in particles size can be overserved and due to sintering at high temperature (700◦C for 4 hours) bigger chunks of particles can be seen which is formed by aggregation (joining) of smaller particles Similar results can be observed in previous research works [153][154].

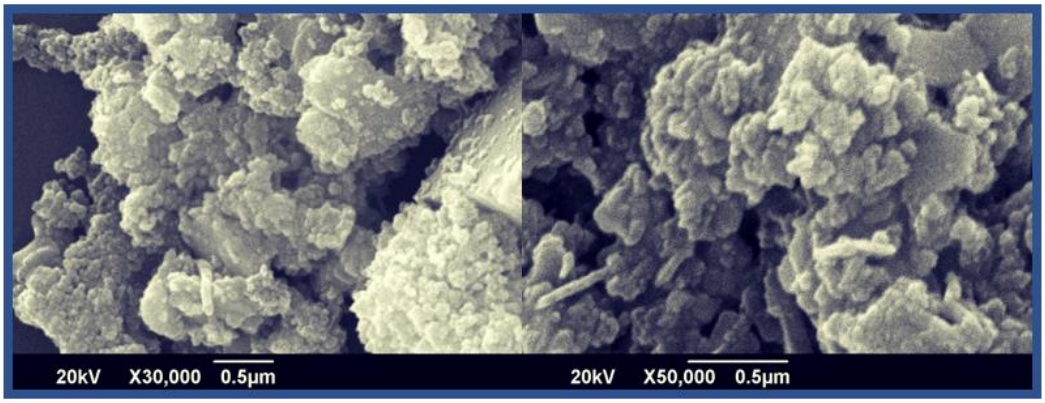

Figure 26: Scanning Electron Microscopy micrographs of $SrFe_2O_4$ nanoparticles

5.3 Energy Dispersive X-Ray (EDX) Composition Analysis:

Elemental analysis was done using energy dispersive spectroscopy (EDX) for the confirmation of doping of strontium to iron oxide nanoparticles. EDX shows $SrFe_2O_4$ prepared at 700 ◦C shows the presence of Strontium (Sr), Iron (Fe) and oxygen (O) as major element present in the structure and their atomic ratios were in accordance to given literature of $SrFe_2O_4$. Impurities peaks that were detected were of gold which is due to gold plating of sample to make it conductive and secondary peak of silicon was observed as the sample was placed on a glass slide due to which small quantity of silicon was detected carbon content is also detected due to powder was place on carbon tape to attach it to sample holder for characterization. It can be observed from the results strontium content increases from 7.7 atomic% to 39.7 atomic% with increase in doping ratio of strontium from 0.25 to 1 mole which corresponds to previous research works[154].

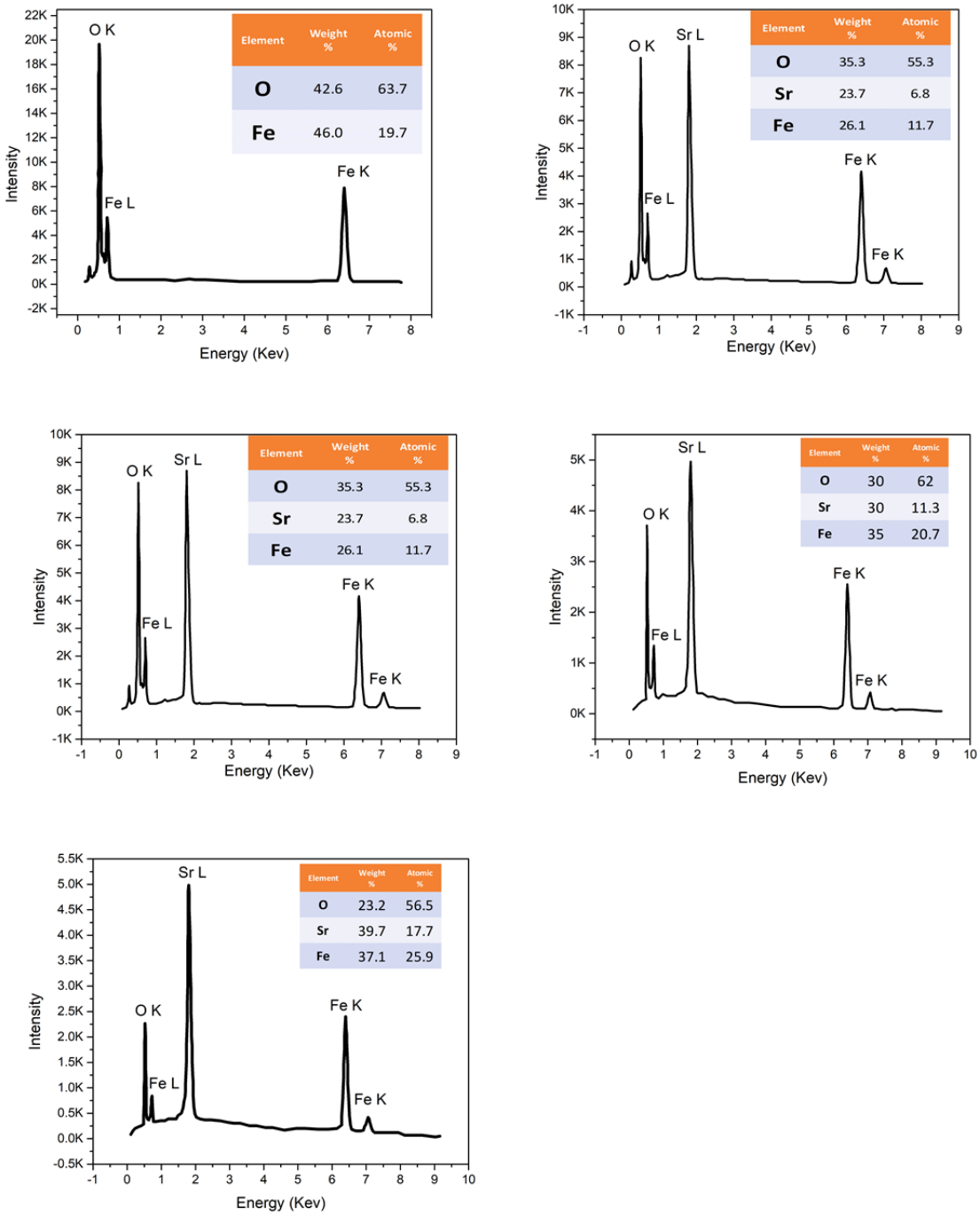

Figure 27: EDX graphs of *Fe_3O_4* ***(A),*** *$Sr_{0.25}Fe_{2.75}O_4$* ***(B),*** *$Sr_{0.5}Fe_{2.5}O_4$* ***(C),*** *$Sr_{0.75}Fe_{2.25}O_4$* ***(D),*** *$SrFe_2O_4$* ***(E)***

5.4 Fourier-Transform Infrared Spectroscopy (FTIR) Analysis:

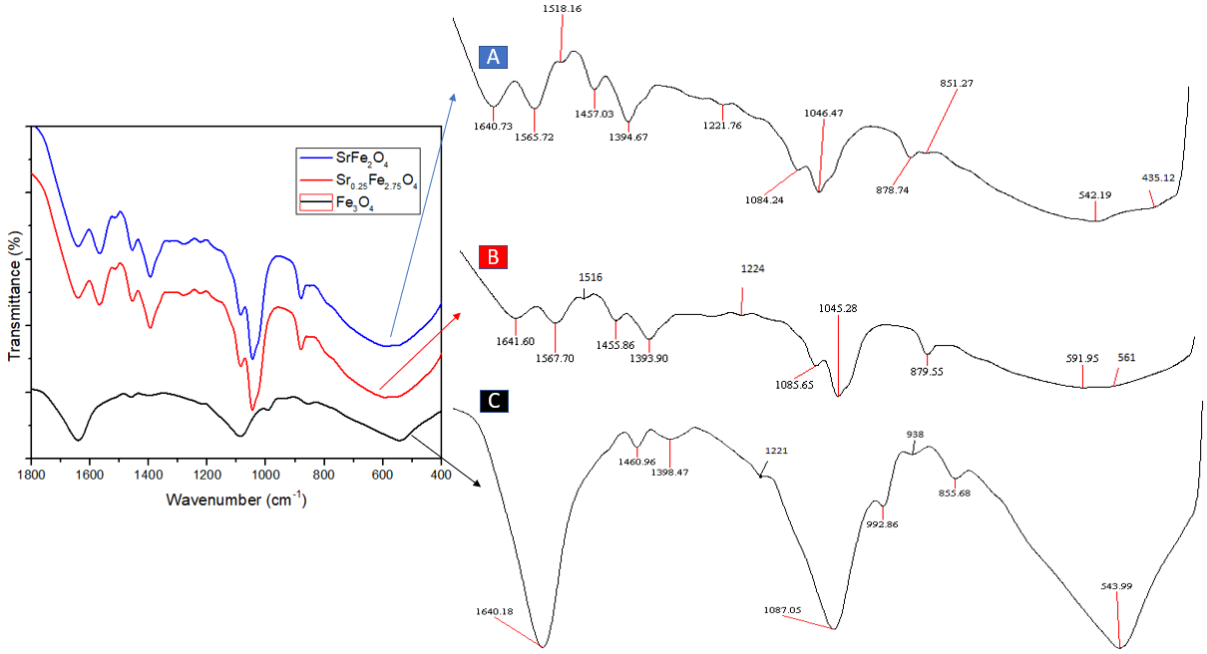

Figure 28: FTIR results of Ibuprofen loaded (A) $SrFe_2O_4$ (B) $Sr_{0.25}Fe_{2.75}O_4$ (C) Fe_3O_4

Figure shows FTIR spectra of Ibuprofen loaded Fe_3O_4(C) $Sr_{0.25}Fe_{2.75}O_4$(B) and $SrFe_2O_4$ (A). In Fe_3O_4 peak at 544cm-1 can be seen which is associated with Fe-O bond stretching in Fe_3O_4 [165]. Peak at 1640 associates to carboxylic group which is related to presence of Ibuprofen on the surface. Absorption band between 900cm-1 to 1100 cm-1 related to bending vibrations associated with O-H bonds. In $SrFe_2O_4$ (A) and $Sr_{0.25}Fe_{2.75}O_4$ (B) bands between 600cm-1 to 400 cm-1 corresponds to formation of tetrahedra and octahedral sites confirming the presence of metal-oxygen stretching band in ferrites. Weak band at 435.12cm-1 associates with octahedral Fe^{+3}-O^{-2} group complex. Bands at 542.16cm-1 (A) and 561 cm-1 (B) corresponds to Fe+3/Sr+2–O group [164]. Bands at 1641cm-1, 1550-1560cm-1,1221-1234cm-1 and 770-900cm-1 are basically foot prints of presence of Ibuprofen in samples corresponding to carboxylic group, νC=C, νC..C and δCH2 groups [163]. These four bands can be identified in all three spectrums hence showing the presence and loading of Ibuprofen molecules.

5.5 Magnetic Properties:

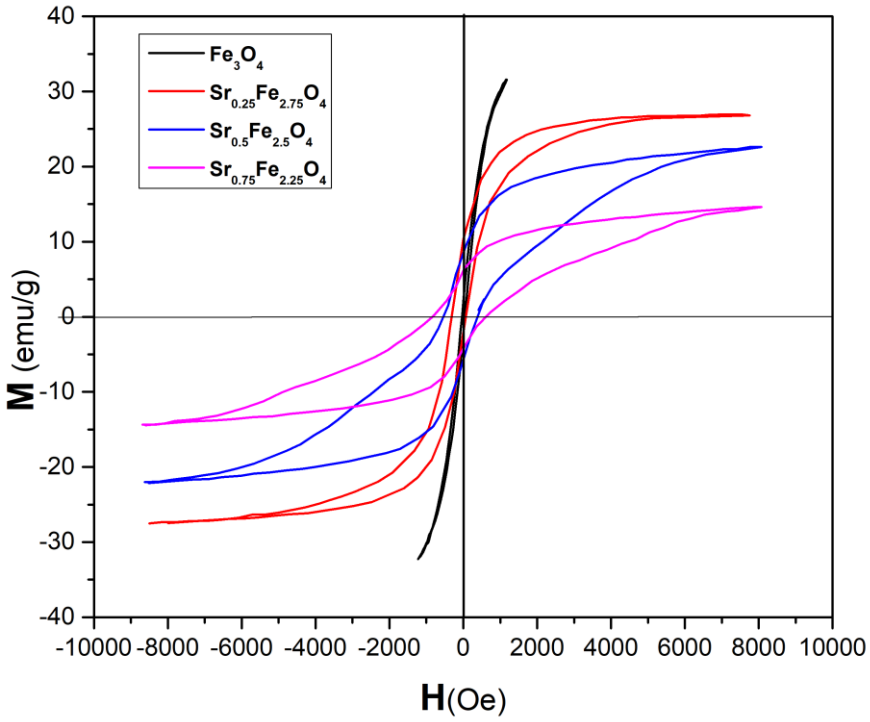

Figure 29: Room Temperature M-H Curve for Nanoparticles

Fig shows the hysteresis loops of Fe3O4 nanoparticles and strontium doped (0.25,0.5 &0.75 molar concentration) Iron oxide nanoparticles, from which magnetic behavior of synthesized nanoparticles can be obtained. Magnetic properties like magnetic coercivity (H_c), saturation magnetization (M_s), isotropic property or squareness ratio (M_r/M_s) and remanence magnetization (M_r), from the hysteresis loops is obtained. It can be observed that with the increase in strontium doping content decrease in saturation magnetization (M_s) can be observed. Increase in magnetic coercivity (H_c) and remanence magnetization (M_r) can be observed which can be associated to shift in magnetic property from soft magnetic material to hard magnetic material. With the increase in strontium content it becomes harder to magnetize and de-magnetize the material hence enhance coercivity is observed. The trend which is observed in previous researches is that up to certain size range (crystallite size) of nanoparticles coercivity increases with increase in size of nanoparticles. Hence similar results are observed in our case. Increase in remanence magnetization is attributed to increase in exchange interaction with increase in strontium content. The squareness ratio of our samples ranges from 0.07 to 0.35 which is less than 0.5, confirming formation of single

domain structure. Superparamagnetic behavior of synthesized Fe3O4 nanoparticles can also be confirmed as squareness ratio is near to zero.

Table 8: Magnetic parameters of Prepared Nanoparticles

Material	M_s (emu/g)	M_r (emu/g)	H_c (Oe)	M_r/M_s	K
Fe_3O_4	34.04	2.25	43.04	0.07	1526.40
$Sr_{0.25}Fe_{2.75}O_4$	28.19	6.43	187.46	0.23	5504.68
$Sr_{0.5}Fe_{2.5}O_4$	22.86	7.39	446.58	0.32	10633.72
$Sr_{0.75}Fe_{2.25}O_4$	14.94	5.20	725.87	0.35	11298.62

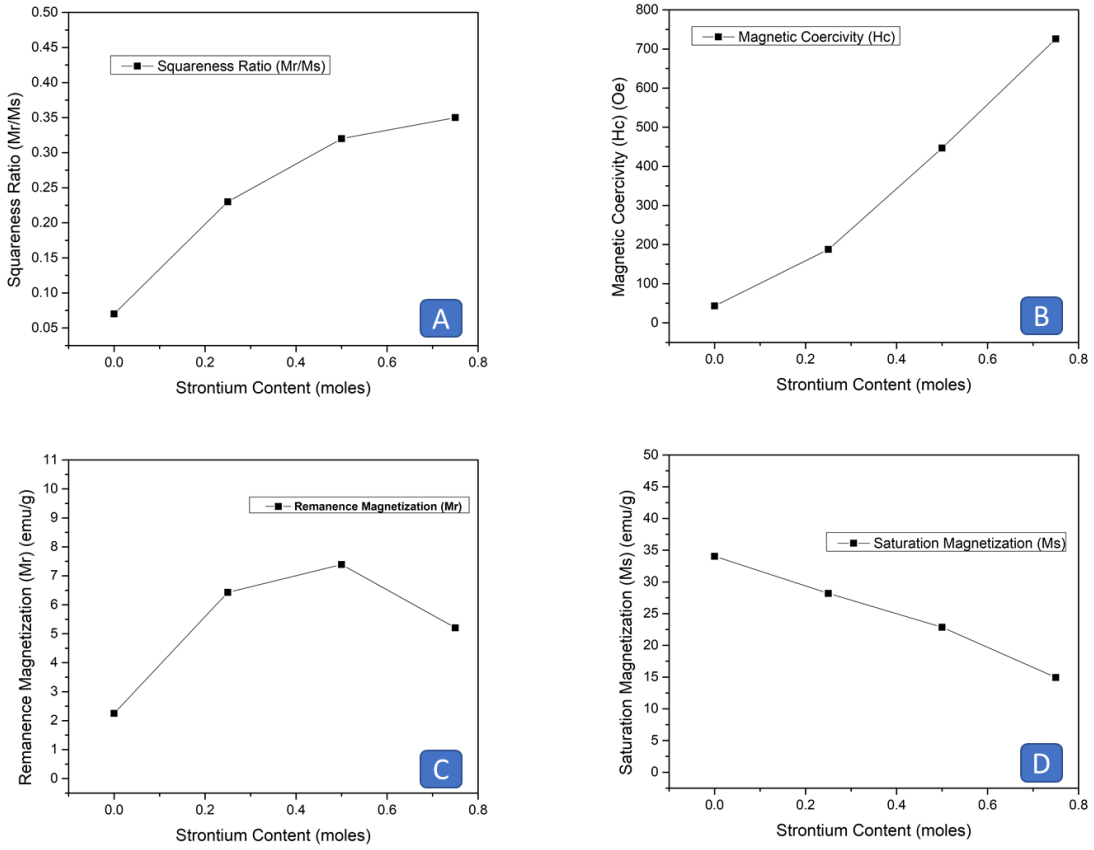

Figure 30: Variation in Squareness Ratio (Mr/Ms) (A) Remanence Magnetization (Mr) (B) Magnetic Coercivity (Hc) (C) Saturation Magnetization (Ms) (D) with increase in Strontium content

5.6 UV Vis Spectroscopy:

5.6.1 Fe_3O_4:

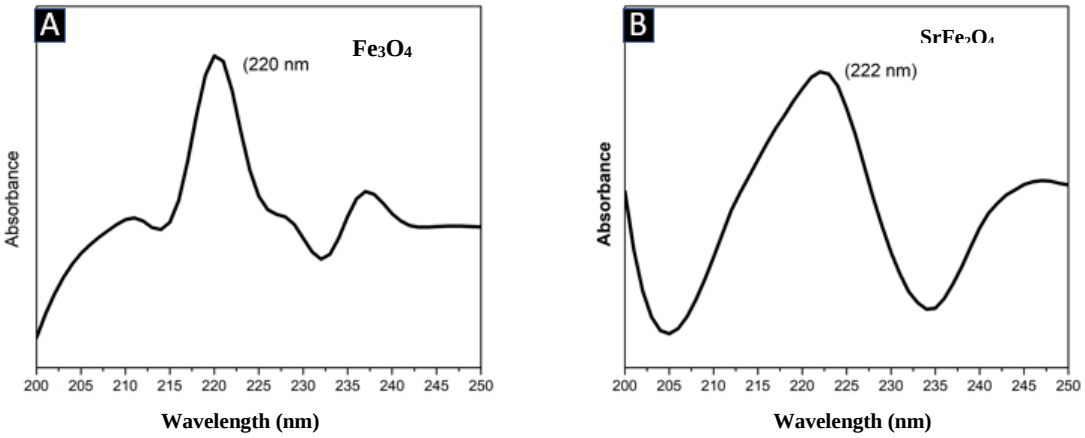

Figure 31: UV Vis Spectra of Fe_3O_4(A) and $SrFe_2O_4$(B) nanoparticles

Figure shows UV Vis spectra of Fe_3O_4 (A) and $SrFe_2O_4$(B) nanoparticles. These particles were observed by dissolving 4 mg of nanoparticles in 4 ml of deionized water to maker 1mg/ml solution. The solution was analyzed using quartz cuvettes. characteristic peak of Fe_3O_4 nanoparticles is observed at 220 nanometer which is in accordance to reference data[155] confirming the formation of magnetite nanoparticles and revealing optical properties having band gap of 5.636 eV. Whereas $SrFe_2O_4$ showed characteristic peak at 222 nanometer which is also in accordance to reference data[154] confirming $SrFe_2O_4$ phase having band gap of 5.58 eV.

5.6.2 Strontium Doped Iron Oxide:

figure below shows the effect of strontium doping on magnetite nanoparticles. The amount strontium doped varies from 0.25 moles ,0.5moles to 0.75 moles. The characteristics peaks of these doped nanoparticles changes as the amount of doping changes. For 0.25 moles of Strontium characteristic peak lies at 223 nanometer and a smaller peak lies at 257 nanometer corresponding to band gap of 5.56eV and 4.82eV. For 0.5 mole of strontium doped nanoparticles, characteristic peak lies at 246 nanometer corresponding to band gap of 5.04ev. and for 0.75 moles of strontium doped nanoparticles characteristic peak is observed at 235 nanometer corresponding to band gap of 5.27eV. Change in particle size can be observed as the smaller the particle sizes the more absorption is toward lower wavelength.

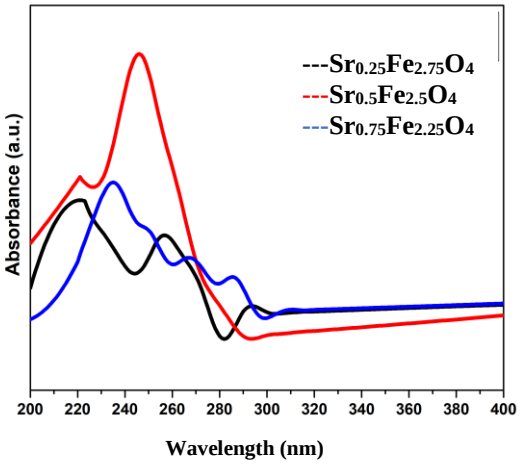

Figure 32: Combined UV Vis spectra of $Sr_{0.25}Fe_{2.75}O_4$***,*** $Sr_{0.5}Fe_{2.5}O_4$ ***and*** $Sr_{0.75}Fe_{2.25}O_4$

5.7 Drug Loading of Nanoparticles:

Iron oxide nanoparticle and strontium doped nanoparticles with strontium content .25, .5, .75 and 1 molar were loaded with ibuprofen. the sample were prepared by loading 15 mg of drug in 10 ml ethanol to make 1.5mg/ml solution. the solution was stirred for 24 hours and then centrifuged. The amount of drug remaining in the solution was detected at 264 nm wavelength us uv- vis spectrophotometer.

5.7.1 Standard Curve of Ibuprofen:

To find the standard curve of Ibuprofen different dilutions were prepared and the graph was plotted between Absorbance and concentration. 0.2mg/ml, 0.3mg/ml, 0.5mg/ml and 0.9 mg/ml solutions were prepared in ethanol to find the standard curve of Ibuprofen. Absorbance was measured at 264 nanometers to detect the amount of drug in terms of absorbance at different dilutions.

Table 9: Absorbance values of Ibuprofen with difference concentration

Concentration	Absorbance		mean
mg/ml	1	2	
0.2	0.4125	0.352	0.38225
0.3	0.5825	0.5423	0.5624
0.5	0.9399	0.879	0.90945
0.9	1.5139	1.66	1.58695

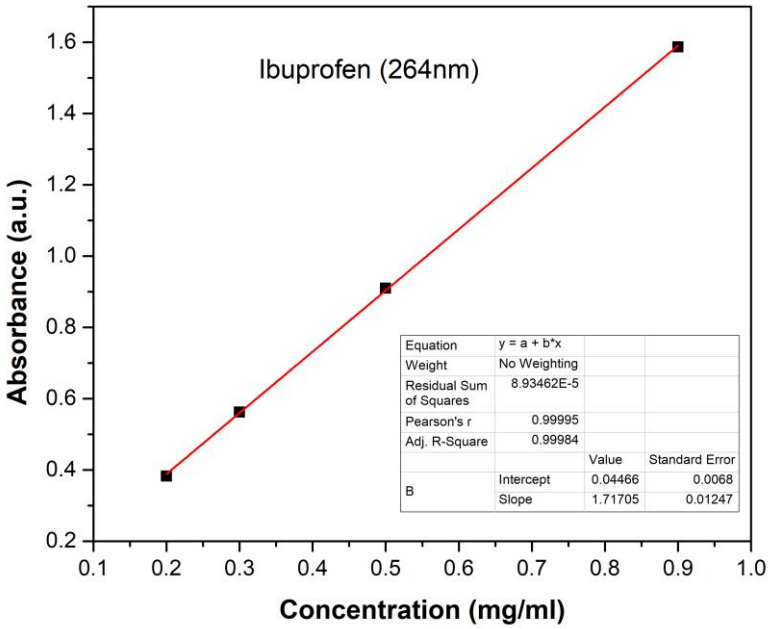

Figure 33: Standard Curve of Ibuprofen

5.7.2 Drug Loading on Nanoparticles:

Encapsulation efficiency of nanoparticles were determined by following formula.

$$Encapsulation\ Efficiency\ (\%) = \frac{Initial\ Drug\ weight - Free\ drug\ weight\ in\ the\ Spernatant}{Initial\ Drug\ weight}$$

Equation 6: Formula for calculating Encapsulation Efficiency[156]

The amount of drug remaining in the supernatant was calculated using absorbance value at 264 nanometer which was then compared to standard curve of Ibuprofen to calculate the amount of drug relative to that absorbance value. The absorbance value of samples at 264 nanometers determine by uv-vis spectrophotometer are shown in the image below.

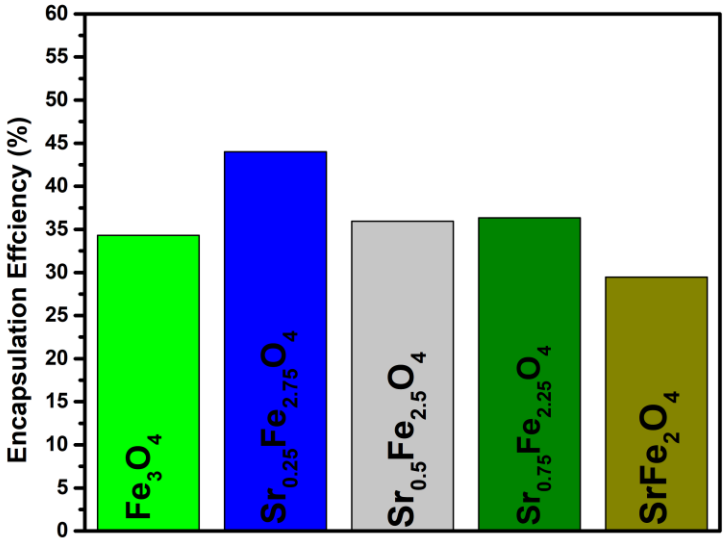

Figure 34: Absorbance of Ibuprofen remaining in the supernatant of different samples

Table 10: Encapsulation Efficiency of Fe_3O_4 and Strontium doped Iron Oxide with Ibuprofen

Sample	Absorbance value	Relative drug weight (mg/ml)	Initial drug weight (mg/ml)	Encapsulation efficiency
Fe_3O_4	1.7266	0.985309427	1.5	**34.31%**
$Sr_{O.25}Fe_{2.75}O_4$	1.475	0.839791787	1.5	**44.01%**
$Sr_{0.5}Fe_{2.5}O_4$	1.684	0.960670908	1.5	**35.96%**
$Sr_{0.75}Fe_{2.25}O_4$	1.6744	0.955118566	1.5	**36.33%**
$SrFe_2O_4$	1.8527	1.058241758	1.5	**29.45%**

Ibuprofen at 1.5 mg/ml have absorbance value 2.6201 which was calculated from standard curve of Ibuprofen shown above. The remaining drug content, detected at 264 nanometers from uv-vis spectrophotometer, was measure by standard cure of Ibuprofen. The relative drug weight was calculated against absorbance values. Fe_3O_4 nanoparticles showed encapsulation efficiency of 34.31% whereas 0.25 moles strontium doped iron oxide nanoparticles showed encapsulation efficiency of 44.01% which is calculated to be highest among all sample's encapsulation efficiencies. The Increase drug loading can be attributed to the fact that strontium is an alkaline earth metal and it creates more basic sites on nanoparticles hence creating enhanced bonding with carboxylic group present in Ibuprofen. Other samples with strontium content 0.5 and 0.75 moles showed encapsulation efficiency

of 35.96% and 36.33% which was better than encapsulation efficiency of Fe_3O_4 alone. The encapsulation efficiency of 0.5 and 0.75 moles doped iron oxide nanoparticles is less than 0.25 moles doped Iron oxide nanoparticles which could be attributed to the fact that particle size increased with the increase in strontium content hence reducing Specific surface area hence reducing the content of drug loaded[157]. In previous studies it has been observed that drug loading depends on many factors including textural properties like pore volume and pore size. Smaller the pore size smaller is the release rate, higher the pore volume, higher will be the amount of drug gets encapsulated. Secondly specific surface area plays an important role in drug loading phenomenon. It has been observed that higher the specific surface area higher will be the amount of drug loaded. Functionalization also enhance the drug loading capabilities. In our case our samples were non-porous and there is no coating or functionalization element, therefore Specific Surface area plays major role in determining drug loading capabilities of these nanoparticulate samples[158][159][160]. Increase in particle size can be observed from SEM results and from crystallite size calculated from XRD results with the help of Scherrer equation. For SEM result it can be observed, with the increase in strontium content increase in overall particle size can be observed and a shift from spherical to rod shape morphology can be seen which is larger in size hence having low specific surface area. It is also observed with increase in strontium content crystallite size increases from 6nm to 13 nm, showing increase in particle size hence decreasing overall specific surface area.

5.7.3 Drug Release Studies of Nanoparticles:

In vitro drug release profile was studied for all drug loaded samples performed for a period of 48h in pH 7.4 phosphate buffer held at 37 °C. The cumulative Concentration (CC) of drug released was calculated with the help of UV vis absorption spectra at 264 nm is shown in table below. It can be observed that for sample $Sr_{0.25}Fe_{2.75}O_4$ maximum amount of drug (0.58 mg/ml) was released with respect to all other samples which is evident from the previous results that $Sr_{0.25}Fe_{2.75}O_4$ showed the maximum encapsulation efficiency among all samples. $Sr_{0.75}Fe_{2.25}O_4$ showed the maximum release percentage of drug of 97.5% with respect to amount of drug loaded on these sample within in the period of 48 hrs. Fe_3O_4 showed minimum percentage of drug released of about 63.15% within 48 hours.

Table 11: Cumulative and percentage drug release data of drug loaded nanoparticles

Time (hrs)	Fe_3O_4		$Sr_{0.25}Fe_{2.75}O_4$		$Sr_{0.5}Fe_{2.5}O_4$		$Sr_{0.75}Fe_{2.25}O_4$		$SrFe_2O_4$	
	CC (mg/ml)	% Released	CC (mg/ml)	% Released	CC (mg/ml)	% Released	CC (mg/ml)	% Released	CC (mg/ml)	% Released
3	0.095142	18.48129	0.276403	41.87917	0.148641	27.5567	0.238924	43.9199	0.111047	25.06135
6	0.128282	24.91885	0.348253	52.76566	0.192435	35.67574	0.301093	55.348	0.152134	34.33405
12	0.161735	31.41708	0.423939	64.23314	0.239335	44.37057	0.350561	64.44136	0.208855	47.13492
24	0.238028	46.23694	0.494002	74.84884	0.293366	54.38749	0.418907	77.00494	0.276125	62.31662
36	0.293916	57.09315	0.54963	83.27725	0.350642	65.00593	0.480052	88.24486	0.341625	77.0989
48	0.325147	63.15996	0.580428	87.94364	0.394757	73.18448	0.530717	97.5583	0.399526	90.16604

Graphs below shows Ibuprofen release profile of all samples. In first 6 hours we can see burst release of drug for all samples. For $Sr_{0.75}Fe_{2.25}O_4$ and $Sr_{0.25}Fe_{2.75}O_4$, 55.3% and 52.76% of loaded drug was released and after that for period of 42 hours, steady amount of drug release is observed for all samples. Graph A shows Cumulative drug release percentage for every samples calculated on the basis of amount of drug loaded on each nanoparticulate samples. It can be observed that during first 3 hours burst release of drug occurred from all samples. Table A shows the drug release percentage of these samples which in basically the ratio of amount of drug released to the amount of drug which actually gets loaded on these samples. Graph B shows the actual cumulative amount of drug released by all samples for the period of 48 hours. In which it can be observed that $Sr_{0.25}Fe_{2.75}O_4$ show highest amount of drug released within the period of 48 hours. It can be observed the release profile of all sample showed better performance with respect to Fe_3O_4 drug release profile.

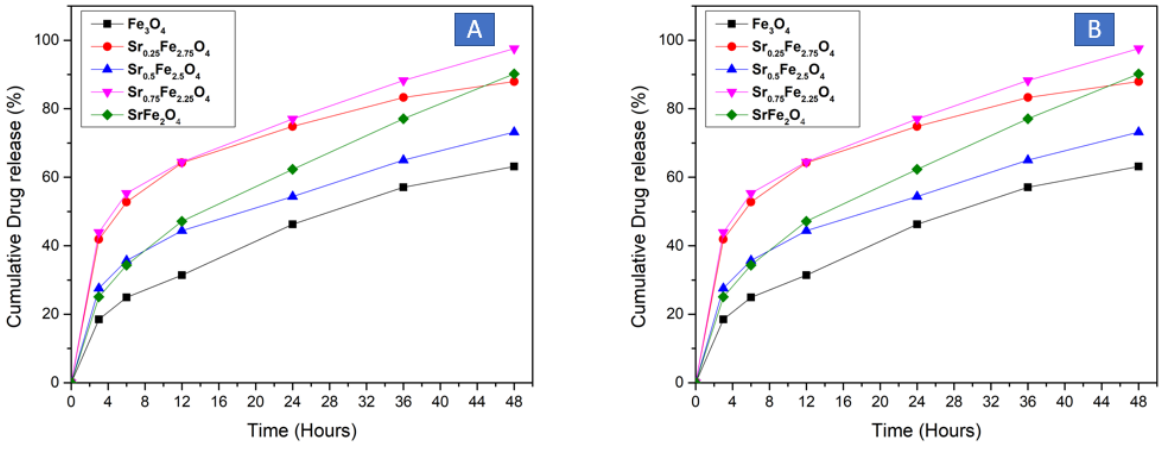

Figure 35: (A) % Cumulative drug release profile of all samples (B) Cummulative Drug Release concentration(mg/ml) for all samples

5.8 Cytotoxicity Results:

To examine the cytotoxic effect of nanoparticles MTT Assay was used. Hep-2 cell line was used to examine cytotoxic effect of magnetite nanoparticles, strontium doped iron oxide nanoparticles and Ibuprofen loaded nanoparticles. Hep-2 cell line was treated with different concentration (300, 400 and 500 µg/ml) of nanoparticles and were incubated for 24 hours to see the cytotoxic effect of these nanoparticles. Decrease in cell viability can be seen with the increase in concentration of nanoparticles. Table show the average values that were obtained by repeating experiment two times. The absorbance values from each well was taken by BioTek Microplate reader. The Cell viability was calculated by comparing values of each cell by the absorbance values of control. The formula used for calculating % cell viability is:

$$\%\ \boldsymbol{Cell\ Viability} = \frac{\boldsymbol{Absorbance\ (sample\ well)}}{\boldsymbol{Absorbance\ (Control\ well)}} \times \mathbf{100}$$

Equation 7: ***Percentage cell viability (%) of different concentrations of nanoparticles***

For 10,000 cells per well, Cell viability was calculated. Results showed increasing trend in cytotoxic effect as the concentration of the particles increases for all samples which is in agreement to previous researches [161][162**].** At higher concentration significant reduction in cell viability can be seen for both magnetite and strontium doped Iron oxide nanoparticles. It can be seen from the results that cell viability of $SrFe_2O_4$ nanoparticles at 300 µg/ml concentration shows maximum cell viability of 112.4% and ibuprofen loaded $Sr_{0.5}Fe_{2.5}O_4$ showed minimum cell viability of 52.9% and maximum cytotoxic effect. As the concentration of nanoparticles increases, increase in cytotoxic effect can be seen and decrease in % cell viability can be observed for both magnetite and strontium doped iron oxide nanoparticles.

Table 12: Percentage cell viability (%) of different concentrations of nanoparticles and Ibuprofen loaded nanoparticle

Material	Concentration (µg/ml)				
	Cell Viability %	300	400	500	300 (Ibuprofen loaded)
Fe_3O_4		105.7	70.3	54.1	60.8
$Sr_{0.25}Fe_{2.75}O_4$		86.7	89.8	69.9	54.4
$Sr_{0.5}Fe_{2.5}O_4$		109.0	84.2	69.6	52.9
$Sr_{0.75}Fe_{2.25}O_4$		108.1	91.6	83.5	74.5
$SrFe_2O_4$		112.4	89.5	61.9	81.6

Graph below shows the comparison of cytotoxicity of all samples at 300, 400 and 500 µg/ml concentration. At 300 µg/ml all $SrFe_2O_4$ showed maximum cell viability of 112.4% whereas $Sr_{0.25}Fe_{2.75}O_4$ showed minimum cell viability of 86.7 %. At 400 µg/ml all $Sr_{0.75}Fe_{2.25}O_4$ showed maximum cell viability of 91.6% whereas Fe_3O_4 showed minimum cell viability of 70.3 %. At 500 µg/ml all $Sr_{0.75}Fe_{2.25}O_4$ showed maximum cell viability of 83.5% whereas Fe_3O_4 showed minimum cell viability of 54.1 %. So, from the following results it can be observed that by doping of strontium to Iron oxide nanoparticle, reduction of cytotoxic effect can be seen at all concentration. Which is due to biocompatible nature of strontium.

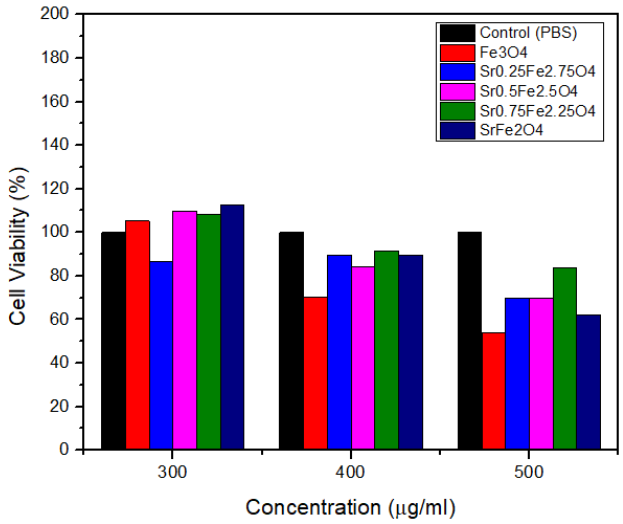

Figure 36: ***The viability of Hep-2 cells after 24 h incubation with nanoparticles of different concentrations according to MTT Assay***

The graph below shows comparison of cytotoxic effect of nanoparticles and Ibuprofen loaded nanoparticles at 300 µg/ml concentration. It can be observed that Ibuprofen Loaded nanoparticles have higher cytotoxic effect with respect to non-loaded nanoparticles at same concentration. For each sample it can be seen that Ibuprofen loaded nanoparticles shows higher cytotoxicity. Ibuprofen loaded $Sr_{0.75}Fe_{2.25}O_4$ nanoparticles showed maximum cytotoxic effect and minimum cell viability of 52.9%. So, it can be observed from the results that Ibuprofen loaded nanoparticles are effective against Hep-2 cancer cell line.

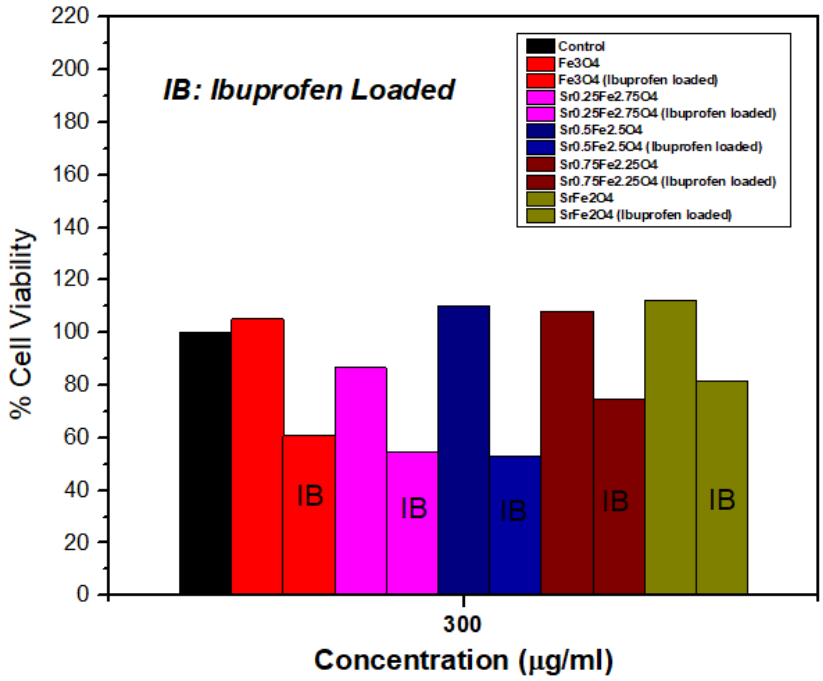

Figure 37: ***Cell viability of Hep-2 cells when treated with nanoparticles and Ibuprofen loaded nanoparticles at 300 µg/ml***

Conclusion

In this study Iron oxide (Fe_3O_4) and Strontium doped (0.25,0.5,0.75 and 1 moles) Iron oxide were developed via coprecipitation method. XRD, EDS results confirmed the formation of strontium doped Iron oxide nanoparticles by showing relevant peaks and confirming different percentages of strontium doped to iron oxide nanoparticles. Nanoparticles synthesized had crystallite sizes ranges from 6-13 nanometer and majority of synthesized nanoparticles were spherical in nature observed by SEM. Ibuprofen was loaded on these nanoparticles in which $Sr_{0.25}Fe_{2.75}O_4$ showed maximum encapsulation efficiency of 44.01%. Result showed by increasing strontium concentration from 0.25 to 1 molar decrease in encapsulation efficiency was observed which was due to reduction in specific surface area due to increase in strontium content. Overall strontium doped Iron oxide nanoparticles showed better drug loading capabilities that Iron oxide nanoparticles. The results of in vitro drug release showed that $Sr_{0.25}Fe_{2.75}O_4$ showed maximum amount of drug released (0.58 mg/ml) in 48 hours, releasing 87% of its loaded drug which was better compared to other nanoparticulate samples. Cytotoxicity (MTT) results showed increase in cytotoxicity with the increase in concentration of nanoparticles. It was observed that with strontium doping, overall cytotoxicity of samples reduces for every concentration. It was also observed Ibuprofen loaded nanoparticles were more cytotoxic to Hep-2 cancer cells with respect to un-loaded nanoparticles. $Sr_{0.25}Fe_{2.75}O_4$ and $Sr_{0.5}Fe_{2.5}O_4$, both loaded with Ibuprofen, showed maximum cytotoxic effect, reducing cell viability to 54.2% and 52.9% of Hep-2 cancer cell line at 300 µg/ml concentration. From Results it can be observed that strontium doped to Iron oxide nanoparticles up to 0.25 molar concentration, improved drug loading capabilities of Iron oxide nanoparticles, showed better drug release profile and higher cytotoxic effects. So strontium doped up to 0.25molar to iron oxide nanoparticle, enhances the properties of Iron oxide nanoparticles for biomedical application, especially in drug delivery applications.

References:

[1] Samrot, A. V., Sahithya, C. S., Selvarani, J., Purayil, S. K., & Ponnaiah, P. (2021). A review on synthesis, characterization and potential biological applications of superparamagnetic iron oxide nanoparticles. Current Research in Green and Sustainable Chemistry, 4, 100042. P.G. Tratnyek, R.L. Johnson, Nanotechnologies for environmental clean-up, Nano Today 1 (2) (2006) 44–48.

[2] Davis, S. S. (1997). Biomedical applications of nanotechnology—implications for drug targeting and gene therapy. Trends in biotechnology, 15(6), 217-224.H.C. Kim,

[3] D.K. Kim, Y. Zhang, W. Voit, K.V. Rao, M. Muhammed, Synthesis and characterization of surfactant-coated superparamagnetic monodispersed iron oxide nanoparticles, J. Magn. Magn Mater. 225 (1–2) (2001) 30–36.'

[4] Wikipedia contributors. *Nanoparticle*. Wikipedia (2022, July 20). https://en.wikipedia.org/wiki/Nanoparticle

[5] Mattox, D. M. (2000). Ion plating—past, present and future. Surface and Coatings technology, 133, 517-521.

[6] Rai-Choudhury, P. (1997). Handbook of microlithography, micromachining, and microfabrication: microlithography (Vol. 39). SPIE press.

[7] Corbierre, M. K., Beerens, J., & Lennox, R. B. (2005). Gold nanoparticles generated by electron beam lithography of gold (I)− thiolate thin films. Chemistry of materials, 17(23), 5774-5779.

[8] Tseng, A. A., Chen, K., Chen, C. D., & Ma, K. J. (2003). Electron beam lithography in nanoscale fabrication: recent development. IEEE Transactions on electronics packaging manufacturing, 26(2), 141-149.

[9] Manfrinato, V. R., Zhang, L., Su, D., Duan, H., Hobbs, R. G., Stach, E. A., & Berggren, K. K. (2013). Resolution limits of electron-beam lithography toward the atomic scale. Nano letters, 13(4), 1555-1558.

[10] Yang, G. W. (2007). Laser ablation in liquids: Applications in the synthesis of nanocrystals. Progress in materials Science, 52(4), 648-698.

[11] Amendola, V., & Meneghetti, M. (2009). Laser ablation synthesis in solution and size manipulation of noble metal nanoparticles. Physical chemistry chemical physics, 11(20), 3805-3821.

[12] P.R. Willmott, J.R. Huber, Pulsed laser vaporization and deposition, Rev. Mod. Phys. 72 (1) (2000) 315.

[13] Veintemillas-Verdaguer, S., Morales, M. P., & Serna, C. J. (1998). Continuous production of γ-Fe2O3 ultrafine powders by laser pyrolysis. Materials Letters, 35(3-4), 227-231.

[14] Ling, D., & Hyeon, T. (2013). Chemical design of biocompatible iron oxide nanoparticles for medical applications. Small, 9(9-10), 1450-1466.

[15] Bomatí-Miguel, O., Mazeina, L., Navrotsky, A., & Veintemillas-Verdaguer, S. (2008). Calorimetric study of maghemite nanoparticles synthesized by laser-induced pyrolysis. Chemistry of Materials, 20(2), 591-598.

[16] Cao, W. (2007). Synthesis of nanomaterials by high energy ball milling. Skyspring Nanomaterials. Inc.: Houston, TX, USA.

[17] Fokina, E. L., Budim, N. I., Kochnev, V. G., & Chernik, G. G. (2004). Planetary mills of periodic and continuous action. Journal of Materials Science, 39(16), 5217-5221.

[18] Zhang, Q., Kano, J., & Saito, F. (2007). Fine grinding of materials in dry systems and mechanochemistry. Handbook of Powder Technology, 12, 509-528.

[19] Ahn, T., Kim, J. H., Yang, H. M., Lee, J. W., & Kim, J. D. (2012). Formation pathways of magnetite nanoparticles by coprecipitation method. The journal of physical chemistry C, 116(10), 6069-6076.

[20] Mosafer, J., Abnous, K., Tafaghodi, M., Jafarzadeh, H., & Ramezani, M. (2017). Preparation and characterization of uniform-sized PLGA nanospheres encapsulated with oleic acid-coated magnetic- Fe_3O_4 nanoparticles for simultaneous diagnostic and therapeutic applications. Colloids and Surfaces A: Physicochemical and Engineering Aspects, 514, 146-154.

[21] G D'Costa, DS Pisal, AVRane; Report on Synthesis of nanoparticles and functionalization: Co precipitation method, 2012.

[22] Hayashi, H., & Hakuta, Y. (2010). Hydrothermal synthesis of metal oxide nanoparticles in supercritical water. Materials, 3(7), 3794-3817.

[23] Rane, A. V., Kanny, K., Abitha, V. K., & Thomas, S. (2018). Methods for synthesis of nanoparticles and fabrication of nanocomposites. In Synthesis of inorganic nanomaterials (pp. 121-139). Woodhead publishing.

[24] Chikan, V., & McLaurin, E. J. (2016). Rapid nanoparticle synthesis by magnetic and microwave heating. Nanomaterials, 6(5), 85.

[25] Palomino, R. L., Miró, A. B., Tenorio, F. N., De Jesús, F. S., Escobedo, C. C., & Ammar, S. (2016). Sonochemical assisted synthesis of SrFe12O19 nanoparticles. Ultrasonics sonochemistry, 29, 470-475.

[26] Revati, K., & Pandey, B. D. (2011). Microbial synthesis of iron-based nanomaterials—A review. Bulletin of Materials Science, 34(2), 191-198.

[27] Iravani, S. (2011). Green synthesis of metal nanoparticles using plants. Green Chemistry, 13(10), 2638-2650.

[28] Thorek, D. L., Chen, A. K., Czupryna, J., & Tsourkas, A. (2006). Superparamagnetic iron oxide nanoparticle probes for molecular imaging. Annals of biomedical engineering, 34(1), 23-38.

[29] Lee, S. J., Cho, J. H., Lee, C., Cho, J., Kim, Y. R., & Park, J. K. (2011). Synthesis of highly magnetic graphite-encapsulated FeCo nanoparticles using a hydrothermal process. Nanotechnology, 22(37), 375603.

[30] Chiang, P. C., Hung, D. S., Wang, J. W., Ho, C. S., & Yao, Y. D. (2007). Engineering water-dispersible FePt nanoparticles for biomedical applications. IEEE transactions on magnetics, 43(6), 2445-2447.

[31] Joshi, H. M., Lin, Y. P., Aslam, M., Prasad, P. V., Schultz-Sikma, E. A., Edelman, R., ... & Dravid, V. P. (2009). Effects of shape and size of cobalt ferrite nanostructures on their MRI contrast and thermal activation. The Journal of Physical Chemistry C, 113(41), 17761-17767.

[32] Doaga, A., Cojocariu, A. M., Amin, W., Heib, F., Bender, P., Hempelmann, R., & Caltun, O. F. (2013). Synthesis and characterizations of manganese ferrites for hyperthermia applications. Materials Chemistry and Physics, 143(1), 305-310.

[33] Zhou, J., Zhao, W. Y., Ma, X., Ju, R. J., Li, X. Y., Li, N., ... & Lu, W. L. (2013). The anticancer efficacy of paclitaxel liposomes modified with mitochondrial targeting conjugate in resistant lung cancer. Biomaterials, 34(14), 3626-3638.

[34] Singamaneni, S., Bliznyuk, V. N., Binek, C., & Tsymbal, E. Y. (2011). Magnetic nanoparticles: recent advances in synthesis, self-assembly and applications. Journal of Materials Chemistry, 21(42), 16819-16845.

[35] Bae, Y. H., & Park, K. (2011). Targeted drug delivery to tumors: myths, reality and possibility. Journal of controlled release, 153(3), 198.

[36] Veiseh, O., Gunn, J. W., & Zhang, M. (2010). Design and fabrication of magnetic nanoparticles for targeted drug delivery and imaging. Advanced drug delivery reviews, 62(3), 284-304.

[37] Sethi, M., & Chakarvarti, S. K. (2015). Hyperthermia techniques for cancer treatment: A review. Int. J. PharmTech Res, 8(6), 292-299.

[38] Jeun, M., Kim, Y. J., Park, K. H., Paek, S. H., & Bae, S. (2013). Physical contribution of Néel and Brown relaxation to interpreting intracellular hyperthermia characteristics using superparamagnetic nanofluids. Journal of nanoscience and nanotechnology, 13(8), 5719-5725.

[39] Giustini, A. J., Petryk, A. A., Cassim, S. M., Tate, J. A., Baker, I., & Hoopes, P. J. (2010). Magnetic nanoparticle hyperthermia in cancer treatment. Nano Life, 1(01n02), 17-32.

[40] Berry, C. C., & Curtis, A. S. (2003). Functionalisation of magnetic nanoparticles for applications in biomedicine. Journal of physics D: Applied physics, 36(13), R198.

[41] Huang, Y., He, S., Cao, W., Cai, K., & Liang, X. J. (2012). Biomedical nanomaterials for imaging-guided cancer therapy. Nanoscale, 4(20), 6135-6149.

[42] Guo, J., Hong, H., Chen, G., Shi, S., Nayak, T. R., Theuer, C. P., ... & Gong, S. (2014). Theranostic unimolecular micelles based on brush-shaped amphiphilic block copolymers for tumor-targeted drug delivery and positron emission tomography imaging. *ACS applied materials & interfaces*, *6*(24), 21769-21779.

[43] Sruthi, P. D., Sahithya, C. S., Justin, C., SaiPriya, C., Bhavya, K. S., Senthilkumar, P., & Samrot, A. V. (2019). Utilization of chemically synthesized super paramagnetic iron oxide nanoparticles in drug delivery, imaging and heavy metal removal. *Journal of Cluster Science*, *30*(1), 11-24.

[44] Fuchigami, T., Kawamura, R., Kitamoto, Y., Nakagawa, M., & Namiki, Y. (2012). A magnetically guided anti-cancer drug delivery system using porous FePt capsules. Biomaterials, 33(5), 1682-1687.

[45] Kim, J. Y., Choi, W. I., Kim, M., & Tae, G. (2013). Tumor-targeting nanogel that can function independently for both photodynamic and photothermal therapy and its synergy from the procedure of PDT followed by PTT. Journal of Controlled Release, 171(2), 113-121.

[46] Paul, T., Basu, S., & Sarkar, K. (2014). SPION-mediated soil DNA extraction and comparative analysis with conventional and commercial kit-based protocol. 3 Biotech, 4(6), 669-677.

[47] Sabale, S., Kandesar, P., Jadhav, V., Komorek, R., Motkuri, R. K., & Yu, X. Y. (2017). Recent developments in the synthesis, properties, and biomedical applications of core/shell superparamagnetic iron oxide nanoparticles with gold. Biomaterials science, 5(11), 2212-2225.

[48] Samrot, A. V., Sahithya, C. S., Selvarani, J., Purayil, S. K., & Ponnaiah, P. Current Research in Green and Sustainable Chemistry.

[49] Bao, F., Yao, J. L., & Gu, R. A. (2009). Synthesis of magnetic Fe2O3/Au core/shell nanoparticles for bioseparation and immunoassay based on surface-enhanced Raman spectroscopy. Langmuir, 25(18), 10782-10787.

[50] Kerans, F. F., Lungaro, L., Azfer, A., & Salter, D. M. (2018). The potential of intrinsically magnetic mesenchymal stem cells for tissue engineering. International journal of molecular sciences, 19(10), 3159.

[51] Li, C., Armstrong, J. P., Pence, I. J., Kit-Anan, W., Puetzer, J. L., Carreira, S. C., ... & Stevens, M. M. (2018). Glycosylated superparamagnetic nanoparticle gradients for osteochondral tissue engineering. Biomaterials, 176, 24-33.

[52] Nikalje, A. P. (2015). Nanotechnology and its applications in medicine. Med chem, 5(2), 081-089.

[53] Arami, H., Khandhar, A., Liggitt, D., & Krishnan, K. M. (2015). In vivo delivery, pharmacokinetics, biodistribution and toxicity of iron oxide nanoparticles. Chemical Society Reviews, 44(23), 8576-8607.

[54] Senyei, A., Widder, K., & Czerlinski, G. (1978). Magnetic guidance of drug-carrying microspheres. Journal of Applied Physics, 49(6), 3578-3583.

[55] McNamara, K., & Tofail, S. A. (2015). Nanosystems: the use of nanoalloys, metallic, bimetallic, and magnetic nanoparticles in biomedical applications. Physical chemistry chemical physics, 17(42), 27981-27995.

[56] Reddy, L. H., Arias, J. L., Nicolas, J., & Couvreur, P. (2012). Magnetic nanoparticles: design and characterization, toxicity and biocompatibility, pharmaceutical and biomedical applications. Chemical reviews, 112(11), 5818-5878.

[57] Sun, C., Lee, J. S., & Zhang, M. (2008). Magnetic nanoparticles in MR imaging and drug delivery. Advanced drug delivery reviews, 60(11), 1252-1265.

[58] Ren, G., Ding, H., Li, Y., & Lu, A. (2016). Natural hematite as a low-cost and earth-abundant cathode material for performance improvement of microbial fuel cells. Catalysts, 6(10), 157.

[59] Mahmoudi, M., Sant, S., Wang, B., Laurent, S., & Sen, T. (2011). Superparamagnetic iron oxide nanoparticles (SPIONs): development, surface modification and applications in chemotherapy. Advanced drug delivery reviews, 63(1-2), 24-46.

[60] Wu, M., Zhang, D., Zeng, Y., Wu, L., Liu, X., & Liu, J. (2015). Nanocluster of superparamagnetic iron oxide nanoparticles coated with poly (dopamine) for magnetic field-targeting, highly sensitive MRI and photothermal cancer therapy. Nanotechnology, 26(11), 115102.

[61] Maleki, H., Simchi, A., Imani, M., & Costa, B. F. O. (2012). Size-controlled synthesis of superparamagnetic iron oxide nanoparticles and their surface coating by gold for biomedical applications. Journal of Magnetism and Magnetic Materials, 324(23), 3997-4005.

[62] Faraji, M., Yamini, Y., & Rezaee, M. (2010). Magnetic nanoparticles: synthesis, stabilization, functionalization, characterization, and applications. Journal of the Iranian Chemical Society, 7(1), 1-37.

[63] Teja, A. S., & Koh, P. Y. (2009). Synthesis, properties, and applications of magnetic iron oxide nanoparticles. Progress in crystal growth and characterization of materials, 55(1-2), 22-45.

[64] Rafi, M. M., Ahmed, K., Nazeer, K. P., Siva Kumar, D., & Thamilselvan, M. (2015). Synthesis, characterization and magnetic properties of hematite (α-Fe2O3) nanoparticles on polysaccharide templates and their antibacterial activity. Applied Nanoscience, 5(4), 515-520.

[65] Klotz, S., Steinle-Neumann, G., Strässle, T., Philippe, J., Hansen, T., & Wenzel, M. J. (2008). Magnetism and the Verwey transition in Fe 3 O 4 under pressure. Physical Review B, 77(1), 012411.

[66] Singh, H., Du, J., Singh, P., Mavlonov, G. T., & Yi, T. H. (2018). Development of superparamagnetic iron oxide nanoparticles via direct conjugation with ginsenosides and its in-vitro study. Journal of Photochemistry and Photobiology B: Biology, 185, 100-110.

[67] Zysler, R. D., Fiorani, D., & Testa, A. M. (2001). Investigation of magnetic properties of interacting Fe2O3 nanoparticles. Journal of magnetism and magnetic materials, 224(1), 5-11.

[68] Cornell, R. M., & Schwertmann, U. (2003). The iron oxides: structure, properties, reactions, occurrences, and uses (Vol. 664). Weinheim: Wiley-vch.

[69] Hildebrandt, B., Wust, P., Ahlers, O., Dieing, A., Sreenivasa, G., Kerner, T., ... & Riess, H. (2002). The cellular and molecular basis of hyperthermia. Critical reviews in oncology/hematology, 43(1), 33-56.

[70] Champagne, P. O., Westwick, H., Bouthillier, A., & Sawan, M. (2018). Colloidal stability of superparamagnetic iron oxide nanoparticles in the central nervous system: a review. Nanomedicine, 13(11), 1385-1400.

[71] Samrot, A. V., Sahithya, C. S., Selvarani, J., Purayil, S. K., & Ponnaiah, P. Current Research in Green and Sustainable Chemistry.

[72] Blanco-Mantecon, M., & O'Grady, K. (2006). Interaction and size effects in magnetic nanoparticles. Journal of Magnetism and Magnetic Materials, 296(2), 124-133.

[73] Mahmoudi, M., Laurent, S., Shokrgozar, M. A., & Hosseinkhani, M. (2011). Toxicity evaluations of superparamagnetic iron oxide nanoparticles: cell "vision" versus physicochemical properties of nanoparticles. ACS nano, 5(9), 7263-7276.

[74] Kievit, F. M., & Zhang, M. (2011). Surface engineering of iron oxide nanoparticles for targeted cancer therapy. Accounts of chemical research, 44(10), 853-862.

[75] Kandasamy, G., & Maity, D. (2015). Recent advances in superparamagnetic iron oxide nanoparticles (SPIONs) for in vitro and in vivo cancer nanotheranostics. International journal of pharmaceutics, 496(2), 191-218.

[76] Sun, Y. P., Li, X. Q., Cao, J., Zhang, W. X., & Wang, H. P. (2006). Characterization of zero-valent iron nanoparticles. Advances in colloid and interface science, 120(1-3), 47-56.

[77] Samrot, A. V., SaiPriya, C., Selvarani, J., PJ, J. C., Lavanya, Y., Soundarya, P., ... & Varghese, R. J. (2020). A study on influence of superparamagnetic iron oxide nanoparticles (SPIONs) on green gram (Vigna radiata L.) and earthworm (Eudrilus eugeniae L.). Materials Research Express, 7(5), 055002.

[78] Wang, L., Wang, L., Ding, W., & Zhang, F. (2010). Acute toxicity of ferric oxide and zinc oxide nanoparticles in rats. Journal of nanoscience and nanotechnology, 10(12), 8617-8624.

[79] Li, L., Jiang, L. L., Zeng, Y., & Liu, G. (2013). Toxicity of superparamagnetic iron oxide nanoparticles: research strategies and implications for nanomedicine. Chinese Physics B, 22(12), 127503.

[80] Hamley, I. W. (2003). Nanotechnology with soft materials. Angewandte Chemie International Edition, 42(15), 1692-1712.

[81] Bi, L., Hu, J., Jiang, P., Kim, H. S., Kim, D. H., Onbasli, M. C., ... & Ross, C. A. (2013). Magneto-optical thin films for on-chip monolithic integration of non-reciprocal photonic devices. Materials, 6(11), 5094-5117.

[82] Bautista, M. C., Bomati-Miguel, O., Zhao, X., Morales, M. P., Gonzalez-Carreno, T., de Alejo, R. P., ... & Veintemillas-Verdaguer, S. (2004). Comparative study of ferrofluids based on dextran-coated iron oxide and metal nanoparticles for contrast agents in magnetic resonance imaging. Nanotechnology, 15(4), S154.

[83] Nam, J., Won, N., Bang, J., Jin, H., Park, J., Jung, S., ... & Kim, S. (2013). Surface engineering of inorganic nanoparticles for imaging and therapy. Advanced drug delivery reviews, 65(5), 622-648.

[84] Gupta, A. K., Naregalkar, R. R., Vaidya, V. D., & Gupta, M. (2007). Recent advances on surface engineering of magnetic iron oxide nanoparticles and their biomedical applications.

[85] Gupta, A. K., & Curtis, A. S. (2004). Surface modified superparamagnetic nanoparticles for drug delivery: interaction studies with human fibroblasts in culture. Journal of Materials Science: Materials in Medicine, 15(4), 493-496.

[86] Fahmy, H. M., Mohamed, F. M., Marzouq, M. H., Mustafa, A. B. E. D., Alsoudi, A. M., Ali, O. A., ... & Mahmoud, F. A. (2018). Review of green methods of iron nanoparticles synthesis and applications. BioNanoScience, 8(2), 491-503.

[87] Thorn, C. F., Oshiro, C., Marsh, S., Hernandez-Boussard, T., McLeod, H., Klein, T. E., & Altman, R. B. (2011). Doxorubicin pathways: pharmacodynamics and adverse effects. Pharmacogenetics and genomics, 21(7), 440.

[88] Kampan, N. C., Madondo, M. T., McNally, O. M., Quinn, M., & Plebanski, M. (2015). Paclitaxel and its evolving role in the management of ovarian cancer. BioMed research international, 2015.

[89] Konstat-Korzenny, E., Ascencio-Aragón, J. A., Niezen-Lugo, S., & Vázquez-López, R. (2018). Artemisinin and its synthetic derivatives as a possible therapy for cancer. Medical Sciences, 6(1), 19.

[90] de Sousa Cavalcante, L., & Monteiro, G. (2014). Gemcitabine: metabolism and molecular mechanisms of action, sensitivity and chemoresistance in pancreatic cancer. European journal of pharmacology, 741, 8-16.

[91] Chen, D., Frezza, M., Schmitt, S., Kanwar, J., & P Dou, Q. (2011). Bortezomib as the first proteasome inhibitor anticancer drug: current status and future perspectives. Current cancer drug targets, 11(3), 239-253.

[92] Dasari, S., & Tchounwou, P. B. (2014). Cisplatin in cancer therapy: molecular mechanisms of action. European journal of pharmacology, 740, 364-378.

[93] Herbst, R. S., & Khuri, F. R. (2003). Mode of action of docetaxel–a basis for combination with novel anticancer agents. Cancer treatment reviews, 29(5), 407-415.

[94] Xie, J., Chen, K., Huang, J., Lee, S., Wang, J., Gao, J., ... & Chen, X. (2010). PET/NIRF/MRI triple functional iron oxide nanoparticles. Biomaterials, 31(11), 3016-3022.

[95] Quan, Q., Xie, J., Gao, H., Yang, M., Zhang, F., Liu, G., ... & Chen, X. (2011). HSA coated iron oxide nanoparticles as drug delivery vehicles for cancer therapy. Molecular pharmaceutics, 8(5), 1669-1676.

[96] Xie, J., Wang, J., Niu, G., Huang, J., Chen, K., Li, X., & Chen, X. (2010). Human serum albumin coated iron oxide nanoparticles for efficient cell labeling. Chemical Communications, 46(3), 433-435.

[97] Huang, Y., Mao, K., Zhang, B., & Zhao, Y. (2017). Superparamagnetic iron oxide nanoparticles conjugated with folic acid for dual target-specific drug delivery and MRI in cancer theranostics. Materials Science and Engineering: C, 70, 763-771.

[98] Yang, Y., Guo, Q., Peng, J., Su, J., Lu, X., Zhao, Y., & Qian, Z. (2016). Doxorubicin-conjugated heparin-coated superparamagnetic iron oxide nanoparticles for combined anticancer drug delivery and magnetic resonance imaging. Journal of biomedical nanotechnology, 12(11), 1963-1974.

[99] Estelrich, J., Escribano, E., Queralt, J., & Busquets, M. A. (2015). Iron oxide nanoparticles for magnetically-guided and magnetically-responsive drug delivery. International journal of molecular sciences, 16(4), 8070-8101.

[100] Issa, B., Obaidat, I. M., Albiss, B. A., & Haik, Y. (2013). Magnetic nanoparticles: surface effects and properties related to biomedicine applications. International journal of molecular sciences, 14(11), 21266-21305.

[101] Wagstaff, A. J., Brown, S. D., Holden, M. R., Craig, G. E., Plumb, J. A., Brown, R. E., ... & Wheate, N. J. (2012). Cisplatin drug delivery using gold-coated iron oxide nanoparticles for enhanced tumour targeting with external magnetic fields. Inorganica Chimica Acta, 393, 328-333.

[102] Hornung, A., Poettler, M., Friedrich, R. P., Zaloga, J., Unterweger, H., Lyer, S., ... & Janko, C. (2015). Treatment efficiency of free and nanoparticle-loaded mitoxantrone for magnetic drug targeting in multicellular tumor spheroids. Molecules, 20(10), 18016-18030.

[103] Nadeem, M., Ahmad, M., Akhtar, M. S., Shaari, A., Riaz, S., Naseem, S., ... & Saeed, M. A. (2016). Magnetic properties of polyvinyl alcohol and doxorubicine loaded iron oxide nanoparticles for anticancer drug delivery applications. PloS one, 11(6), e0158084.

[104] Zaloga, J., Janko, C., Nowak, J., Matuszak, J., Knaup, S., Eberbeck, D., ... & Alexiou, C. (2014). Development of a lauric acid/albumin hybrid iron oxide nanoparticle system with improved biocompatibility. International journal of nanomedicine, 9, 4847.

[105] Natesan, S., Ponnusamy, C., Sugumaran, A., Chelladurai, S., Palaniappan, S. S., & Palanichamy, R. (2017). Artemisinin loaded chitosan magnetic nanoparticles for the efficient targeting to the breast cancer. International journal of biological macromolecules, 104, 1853-1859.

[106] Thapa, D., Palkar, V. R., Kurup, M. B., & Malik, S. K. (2004). Properties of magnetite nanoparticles synthesized through a novel chemical route. Materials Letters, 58(21), 2692-2694.

[107] Veiseh, O., Gunn, J. W., & Zhang, M. (2010). Design and fabrication of magnetic nanoparticles for targeted drug delivery and imaging. Advanced drug delivery reviews, 62(3), 284-304.

[108] Jeon, H., Kim, J., Lee, Y. M., Kim, J., Choi, H. W., Lee, J., ... & Kim, W. J. (2016). Poly-paclitaxel/cyclodextrin-SPION nano-assembly for magnetically guided drug delivery system. Journal of Controlled Release, 231, 68-76.

[109] Lee, G. Y., Qian, W. P., Wang, L., Wang, Y. A., Staley, C. A., Satpathy, M., ... & Yang, L. (2013). Theranostic nanoparticles with controlled release of gemcitabine for targeted therapy and MRI of pancreatic cancer. ACS nano, 7(3), 2078-2089.

[110] Mu, Q., Kievit, F. M., Kant, R. J., Lin, G., Jeon, M., & Zhang, M. (2015). Anti-HER2/neu peptide-conjugated iron oxide nanoparticles for targeted delivery of paclitaxel to breast cancer cells. Nanoscale, 7(43), 18010-18014.

[111] Ahmed, M. S. U., Salam, A. B., Yates, C., Willian, K., Jaynes, J., Turner, T., & Abdalla, M. O. (2017). Double-receptor-targeting multifunctional iron oxide nanoparticles drug delivery system for the treatment and imaging of prostate cancer. International Journal of Nanomedicine, 12, 6973.

[112] Nagesh, P. K., Johnson, N. R., Boya, V. K., Chowdhury, P., Othman, S. F., Khalilzad-Sharghi, V., ... & Yallapu, M. M. (2016). PSMA targeted docetaxel-loaded superparamagnetic iron oxide nanoparticles for prostate cancer. Colloids and Surfaces B: Biointerfaces, 144, 8-20.

[113] Leach, J. C., Wang, A., Ye, K., & Jin, S. (2016). A RNA-DNA hybrid aptamer for nanoparticle-based prostate tumor targeted drug delivery. International journal of molecular sciences, 17(3), 380.

[114] Arias, L. S., Pessan, J. P., Vieira, A. P. M., Lima, T. M. T. D., Delbem, A. C. B., & Monteiro, D. R. (2018). Iron oxide nanoparticles for biomedical applications: A perspective on synthesis, drugs, antimicrobial activity, and toxicity. Antibiotics, 7(2), 46.

[115] Mura, S., Nicolas, J., & Couvreur, P. (2013). Stimuli-responsive nanocarriers for drug delivery. Nature materials, 12(11), 991-1003.

[116] Kievit, F. M., Wang, F. Y., Fang, C., Mok, H., Wang, K., Silber, J. R., ... & Zhang, M. (2011). Doxorubicin loaded iron oxide nanoparticles overcome multidrug resistance in cancer in vitro. Journal of controlled release, 152(1), 76-83.

[117] Gautier, J., Munnier, E., Paillard, A., Hervé, K., Douziech-Eyrolles, L., Soucé, M., ... & Chourpa, I. (2012). A pharmaceutical study of doxorubicin-loaded PEGylated nanoparticles for magnetic drug targeting. International journal of pharmaceutics, 423(1), 16-25.

[118] Wimardhani, Y. S., Suniarti, D. F., Freisleben, H. J., Wanandi, S. I., Siregar, N. C., & Ikeda, M. A. (2014). Chitosan exerts anticancer activity through induction of apoptosis and cell cycle arrest in oral cancer cells. *Journal of oral science*, *56*(2), 119-126.

[119] Unsoy, G., Yalcin, S., Khodadust, R., Mutlu, P., Onguru, O., & Gunduz, U. (2014). Chitosan magnetic nanoparticles for pH responsive Bortezomib release in cancer therapy. Biomedicine & Pharmacotherapy, 68(5), 641-648.

[120] Unsoy, G., Khodadust, R., Yalcin, S., Mutlu, P., & Gunduz, U. (2014). Synthesis of Doxorubicin loaded magnetic chitosan nanoparticles for pH responsive targeted drug delivery. European Journal of Pharmaceutical Sciences, 62, 243-250.

[121] Adimoolam, M. G., Amreddy, N., Nalam, M. R., & Sunkara, M. V. (2018). A simple approach to design chitosan functionalized Fe_3O_4 nanoparticles for pH

responsive delivery of doxorubicin for cancer therapy. Journal of Magnetism and Magnetic Materials, 448, 199-207.

[122] Zou, Y., Liu, P., Liu, C. H., & Zhi, X. T. (2015). Doxorubicin-loaded mesoporous magnetic nanoparticles to induce apoptosis in breast cancer cells. Biomedicine & Pharmacotherapy, 69, 355-360.

[123] Quinto, C. A., Mohindra, P., Tong, S., & Bao, G. (2015). Multifunctional superparamagnetic iron oxide nanoparticles for combined chemotherapy and hyperthermia cancer treatment. Nanoscale, 7(29), 12728-12736.

[124] Peng, S., Zhou, G., Luk, K. D., Cheung, K. M., Li, Z., Lam, W. M., ... & Lu, W. W. (2009). Strontium promotes osteogenic differentiation of mesenchymal stem cells through the Ras/MAPK signaling pathway. Cellular Physiology and Biochemistry, 23(1-3), 165-174.

[125] Silva, G. A. B., Bertassoli, B. M., Sousa, C. A., Albergaria, J. D., de Paula, R. S., & Jorge, E. C. (2018). Effects of strontium ranelate treatment on osteoblasts cultivated onto scaffolds of trabeculae bovine bone. Journal of bone and mineral metabolism, 36(1), 73-86.

[126] Almeida, M. M., Nani, E. P., Teixeira, L. N., Peruzzo, D. C., Joly, J. C., Napimoga, M. H., & Martinez, E. F. (2016). Strontium ranelate increases osteoblast activity. Tissue and Cell, 48(3), 183-188.

[127] Lode, A., Heiss, C., Knapp, G., Thomas, J., Nies, B., Gelinsky, M., & Schumacher, M. (2018). Strontium-modified premixed calcium phosphate cements for the therapy of osteoporotic bone defects. Acta biomaterialia, 65, 475-485.

[128] Patel, U., Macri-Pellizzeri, L., Zakir Hossain, K. M., Scammell, B. E., Grant, D. M., Scotchford, C. A., ... & Sottile, V. (2019). In vitro cellular testing of strontium/calcium substituted phosphate glass discs and microspheres shows potential for bone regeneration. Journal of Tissue Engineering and Regenerative Medicine, 13(3), 396-405.

[129] Kuo, Y. C., & Chen, C. W. (2017). Neuroregeneration of induced pluripotent stem cells in polyacrylamide-chitosan inverted colloidal crystal scaffolds with poly (lactide-co-glycolide) nanoparticles and transactivator of transcription von Hippel-Lindau peptide. Tissue Engineering Part A, 23(7-8), 263-274.

[130] Elumalai, A. (2020). Using strontium coated clay nanoparticles for bone regeneration and other biomedical applications.

[131] Aimaiti A et al (2017) Low-dose strontium stimulates osteogenesis but high-dose doses cause apoptosis in human adiposederived stem cells via regulation of the ERK1/2 signaling pathway. Stem Cell Res Ther 8(1):1–12

[132] Mousavi SR et al (2019) A novel and reusable magnetic nano catalyst developed based on graphene oxide incorporated strontium nanoparticles for the facial synthesis of β-enamino ketones under solvent-free conditions. Appl Organomet Chem 33(1):e4644

[133] Nichols, J. W., & Bae, Y. H. (2014). EPR: Evidence and fallacy. Journal of Controlled Release, 190, 451-464.

[134] Ulbrich, K., Hola, K., Subr, V., Bakandritsos, A., Tucek, J., & Zboril, R. (2016). Targeted drug delivery with polymers and magnetic nanoparticles: covalent and noncovalent approaches, release control, and clinical studies. Chemical reviews, 116(9), 5338-5431.

[135] Chillistone S, Hardman JG (2017) Factors affecting drug absorption and distribution. Anaesth Intensive Care Med 18(7):335–339

[136] Vertzoni M et al (2019) Impact of regional differences along the gastrointestinal tract of healthy adults on oral drug absorption: an UNGAP review. Eur J Pharm Sci 134:153–175

[137] Filippousi M et al (2015) Modified chitosan coated mesoporous strontium hydroxyapatite nanorods as drug carriers. J Mater Chem B 3(29):5991–6000

[138] Zhang J et al (2012) Novel mesoporous hydroxyapatite/chitosan composite for bone repair. J Bionic Eng 9(2):243–251

[139] Zhang C et al (2010) Self-activated luminescent and mesoporous strontium hydroxyapatite nanorods for drug delivery. Biomaterials 31(12):3374–3383

[140] Kiani FA et al (2018) Optimization of Ag2O nanostructures with strontium for biological and therapeutic potential. Artif Cells Nanomed Biotechnol 46(sup3):S1083–S1091

[141] Qian W-Y et al (2012) pH-sensitive strontium carbonate nanoparticles as new anticancer vehicles for controlled etoposide release. Int J Nanomed 7:5781

[142] Smith DM, Simon JK, Baker JR Jr (2013) Applications of nanotechnology for immunology. Nat Rev Immunol 13(8):592–605

[143] Garbani M et al (2017) Allergen-loaded strontium-doped hydroxyapatite spheres improve allergen-specific immunotherapy in mice. Allergy 72(4):570–578

[144] Khamsehashari N, Hassanzadeh-Tabrizi S, Bigham A (2018) Effects of strontium adding on the drug delivery behaviour of silica nanoparticles synthesized by P123-assisted sol–gel method. Mater Chem Phys 205:283–291

[145] Yurtdaş-Kırımlıoğlu, G., Görgülü, Ş., & Berkman, M. S. (2020). Novel approaches to cancer therapy with ibuprofen-loaded Eudragit® RS 100 and/or octadecylamine-modified PLGA nanoparticles by assessment of their effects on apoptosis. Drug Development and Industrial Pharmacy, 46(7), 1133-1149.

[146] Harris, R. E., Beebe-Donk, J., Doss, H., & Doss, D. B. (2005). Aspirin, ibuprofen, and other non-steroidal anti-inflammatory drugs in cancer prevention: a critical review of non-selective COX-2 blockade. Oncology reports, 13(4), 559-583.

[147] Endo, H., Yano, M., Okumura, Y., & Kido, H. (2014). Ibuprofen enhances the anticancer activity of cisplatin in lung cancer cells by inhibiting the heat shock protein 70. Cell death & disease, 5(1), e1027-e1027.

[148] Patil, R. M., Thorat, N. D., Shete, P. B., Bedge, P. A., Gavde, S., Joshi, M. G., ... & Bohara, R. A. (2018). Comprehensive cytotoxicity studies of superparamagnetic iron oxide nanoparticles. Biochemistry and biophysics reports, 13, 63-72.

[149] Mahdavi, M., Ahmad, M. B., Haron, M. J., Namvar, F., Nadi, B., Rahman, M. Z. A., & Amin, J. (2013). Synthesis, surface modification and characterisation of biocompatible magnetic iron oxide nanoparticles for biomedical applications. *Molecules*, *18*(7), 7533-7548.

[150] Berthet, P., Berthon, J., Heger, G., & Revcolevschi, A. (1992). Structure of metastable strontium ferrite. Materials research bulletin, 27(8), 919-924.

[151] Singh, Sukhdeep. (2014). Hydrothermal synthesis of NiFe2O4, Ni0.6Zn0.4Fe2O4 and Ni0.6Zn0.4Fe2O4/$SrFe_2O_4$: nanostructure, magnetic and dielectric properties. Indian Journal of Pure and Applied Physics. 52. 550-555.

[152] Al-Maswari, B. M., Al-Zaqri, N., Ahmed, J., Ahamad, T., Boshaala, A., Ananda, S., & Venkatesha, B. M. (2022). Nanomagnetic strontium ferrite nitrogen doped carbon ($SrFe_2O_4$-NC): Synthesis, characterization and excellent supercapacitor performance. Journal of Energy Storage, 52, 104821

[153] Ghahfarokhi, S. M., & Shobegar, E. M. (2020). Influence of pH on the structural, magnetic and optical properties of $SrFe_2O_4$ nanoparticles. Journal of Materials Research and Technology, 9(6), 12177-12186.

[154] Ghahfarokhi, S. E., Shobegar, E. M., & Shoushtari, M. Z. (2021). Preparation and characterization of spinel $SrFe_2O_4$ nanoparticles by method sol-gel. *Journal of the Australian Ceramic Society*, *57*(5), 1359-1369.

[155] Villegas, V. A. R., Ramírez, J. I. D. L., Guevara, E. H., Sicairos, S. P., Ayala, L. A. H., & Sanchez, B. L. (2020). Synthesis and characterization of magnetite nanoparticles for photocatalysis of nitrobenzene. *Journal of Saudi Chemical Society*, *24*(2), 223-235.

[156] Patil, R. M., Thorat, N. D., Shete, P. B., Bedge, P. A., Gavde, S., Joshi, M. G., ... & Bohara, R. A. (2018). Comprehensive cytotoxicity studies of superparamagnetic iron oxide nanoparticles. Biochemistry and biophysics reports, 13, 63-72.

[157] Khamsehashari, N., Hassanzadeh-Tabrizi, S. A., & Bigham, A. (2018). Effects of strontium adding on the drug delivery behavior of silica nanoparticles synthesized by P123-assisted sol-gel method. Materials Chemistry and Physics, 205, 283-291.

[158] Vallet-Regi, M., Rámila, A., Del Real, R. P., & Pérez-Pariente, J. (2001). A new property of MCM-41: drug delivery system. Chemistry of Materials, 13(2), 308-311.

[159] Tabia, Z., El Mabrouk, K., Bricha, M., & Nouneh, K. (2019). Mesoporous bioactive glass nanoparticles doped with magnesium: drug delivery and acellular in vitro bioactivity. RSC advances, 9(22), 12232-12246.

[160] Doadrio, A. L., Sánchez-Montero, J. M., Doadrio, J. C., Salinas, A. J., & Vallet-Regí, M. (2014). A molecular model to explain the controlled release from SBA-15 functionalized with APTES. Microporous and mesoporous materials, 195, 43-49.

[161] Norouzi, M., Yathindranath, V., Thliveris, J. A., Kopec, B. M., Siahaan, T. J., & Miller, D. W. (2020). Doxorubicin-loaded iron oxide nanoparticles for glioblastoma therapy: A combinational approach for enhanced delivery of nanoparticles. Scientific reports, 10(1), 1-18.

[162] Kanagesan, S., Hashim, M., Tamilselvan, S., Alitheen, N. B., Ismail, I., Hajalilou, A., & Ahsanul, K. (2013). Synthesis, characterization, and cytotoxicity of iron oxide nanoparticles. Advances in Materials Science and Engineering, 2013.

[163] Campos, I., Espindola, A., Chagas, C., Barbosa, E., Castro, C. E., Molina, C., ... & Haddad, P. S. (2020). Biocompatible superparamagnetic nanoparticles with ibuprofen as potential drug carriers. *SN Applied Sciences*, *2*(3), 1-12.

[164] Mousavi Ghahfarokhi, S. E., Mohammadzadeh Shobegar, E., & Zargar Shoushtari, M. (2019). Effects of sintering temperature on structural, morphological and magnetic properties of strontium ferrite nanoparticles. Journal of Superconductivity and Novel Magnetism, 32(4), 1067-1076.

[165] Yusoff, A. H. M., Salimi, M. N., & Jamlos, M. F. (2017, April). Synthesis and characterization of biocompatible Fe3O4 nanoparticles at different pH. In AIP Conference Proceedings (Vol. 1835, No. 1, p. 020010). AIP Publishing LLC.